Neoplasia • Vol. 8, No. 5, May 2006, pp. 373–383

www.neoplasia.com

Gene Expression Profile Related to the Progression of Preneoplastic Nodules toward Hepatocellular Carcinoma in Rats[1*]

Julio Isael Pérez-Carreón, Cristina López-García*, Samia Fattel-Fazenda*, Evelia Arce-Popoca*, Leticia Alemán-Lazarini*, Sergio Hernández-García*, Véronique Le Berre†, Sergueï Sokol†, Jean Marie Francois† and Saúl Villa-Treviño**

*Departamento de Biología Celular, Centro de Investigación y de Estudios Avanzados del IPN, Mexico, DF, Mexico; †Transcriptome-Biochips Platform of Genopole Toulouse Midi-Pyrenees, Centre de Bioingenierie Gilbert Durand, UMR-CNRS 5504, UMR-INRA 792, Institut National des Sciences Appliquees F-31077, Toulouse Cedex 04, France

Abstract

In this study, we investigated the time course gene expression profile of preneoplastic nodules and hepatocellular carcinomas (HCC) to define the genes implicated in cancer progression in a resistant hepatocyte model. Tissues that included early nodules (1 month, ENT-1), persistent nodules (5 months, ENT-5), dissected HCC (12 months), and normal livers (NL) from adult rats were analyzed by cDNA arrays including 1185 rat genes. Differential genes were derived in each type of sample (*n* = 3) by statistical analysis. The relationship between samples was described in a Venn diagram for 290 genes. From these, 72 genes were shared between tissues with nodules and HCC. In addition, 35 genes with statistical significance only in HCC and with extreme ratios were identified. Differential expression of 11 genes was confirmed by comparative reverse transcription–polymerase chain reaction, whereas that of 2 genes was confirmed by immunohistochemistry. Members involved in cytochrome *P*450 and second-phase metabolism were downregulated, whereas genes involved in glutathione metabolism were upregulated, implicating a possible role of glutathione and oxidative regulation. We provide a gene expression profile related to the progression of nodules into HCC, which contributes to the understanding of liver cancer development and offers the prospect for chemoprevention strategies or early treatment of HCC.

Neoplasia (2006) **8,** 373–383

Keywords: Hepatocarcinogenesis, transcriptomic, redox control, cancer markers, glutathione metabolism.

Introduction

Hepatocellular carcinoma (HCC) is a cancer that is prevalent worldwide. Detection of serum α-fetoprotein and liver imaging techniques are the conventional methods used for the identification of this malignancy [1–3]. However, these techniques are not reliable for early diagnosis [4]. Early detection of HCC is an important issue because effective treatment of small tumors is possible by surgical resection [5]. The early stages of human and animal hepatocarcinogenesis are characterized by the presence of preneoplastic lesions, namely, nodules that could be useful for the identification of early tumor markers, for the study of liver cancer progression, and for chemopreventive strategies [6,7]. However, human precancerous lesions such as dysplasic nodules are rather difficult to obtain because of their small size, incidental detection, and coexistence with other liver pathologies [8]. Thus, the rat model for hepatocarcinogenesis has been proven important as a tool for the analysis of nodules and liver cancer progression. Chemically induced nodules in the rat liver share several morphologic, biochemical, and molecular characteristics with human dysplasic nodules [9]. In the resistant hepatocyte (RH) model described by Solt and Farber [10] and Farber and Sarma [11], a necrogenic dose of diethylnitrosamine (DEN) induces resistant hepatocytes (RHs) during initiation. These cells can be stimulated to develop rapidly into altered hepatocyte foci and nodules by a selection procedure in which the carcinogen 2-acetylaminofluorene (2-AAF) is administered in combination with partial hepatectomy (PH) [12,13]. With this regime, which induces rapid growth of resistant altered hepatocytes, visible nodules are formed synchronously—some of them displaying sufficient genomic damage and progress to HCC without any additional treatment with the carcinogen.

As with other cancers, HCC is caused by the accumulation of genetic alterations resulting in a distorted expression of

Abbreviations: HCC, hepatocellular carcinoma; DEN, diethylnitrosamine; 2-AAF, 2-acetylaminofluorene; GSTP, glutathione *S*-transferase, placental form; GGT, γ-glutamyl transpeptidase

Address all correspondence to: Saúl Villa Treviño, MD, PhD, Departamento de Biología Celular, Centro de Investigación y de Estudios Avanzados (CINVESTAV). Av. IPN No. 2508, 07360 Mexico, DF, Mexico. E-mail: svilla@cell.cinvestav.mx

[1]This work was supported by CONACYT grant 39525-M, ECOS-ANUIES grant M02-S01, and a fellowship from CONACYT (JIPC 144549).

*This article refers to supplementary material, which is designated by "W" (i.e., Table W1, Figure W1) and is available online at www.bcdecker.com.

 1522-8002/06/$25.00
DOI 10.1593/neo.05841

thousands of genes. Hence, gene expression analysis with DNA microarray methodologies has been successfully used to study cancer development [14,15]. In this study, using a modified RH model, we investigated the time course of expression changes during the progression of nodules toward cancer using Atlas array membranes bearing 1185 well-typified rat genes. By comparing the expression data between tissues with nodules and HCC, we were able to provide a list of selectively expressed genes at different stages and those genes shared in both situations. We showed that some of the differentially regulated genes are involved in glutathione metabolism and redox control, agreeing with the proposition that altered cellular homeostasis may be a predisposing factor for disease progression in rat hepatocarcinogenesis.

Materials and Methods

Animals and Treatments

F344 rats weighing 180–200 g (UPEAL-Cinvestav, Mexico, DF, Mexico) were subjected to a 10-day carcinogen treatment. All experiments followed Institutional Animal Care and Use Committee Guidelines. Rats were initiated with an intraperitoneal dose of DEN (200 mg/kg; Sigma–Aldrich, Toluca, Mexico) and subjected to a modified selection regime 1 week later [6,16]. 2-AFF was administered by gavage at a dose of 25 mg/kg during three consecutive days, beginning on day 7 after initiation. On day 10, rats were subjected to PH. Animals were sacrificed by exsanguination under ether anesthesia at periods from 1 month after initiation up to 24 months. Livers were excised, washed in physiological saline solution, frozen in 2-methyl butane with liquid nitrogen or immersed in RNA*later* (Sigma, St. Louis, MO), and stored at −80°C.

Histologic Analyses

Representative 20-μm thick sections from liver slices were stained for γ-glutamyl transpeptidase (GGT) activity, in accordance with Rutenburg et al. [17]. In addition, 5-μm sections were processed for routine histologic examination using hematoxylin and eosin (H&E) staining. For immunostaining, formalin-fixed paraffin specimens were blocked for 1 hour in 0.1% H_2O_2 in phosphate-buffered saline, pH 7.4. Subsequently, they were incubated with commercial monoclonal antibodies specific to glutathione *S*-transferase, placental form (GSTP; DakoCytomation, Glostrup, Denmark), or anti–cyclin D1 (Cell-Marque, Hotspring, AR) diluted 1:50 and 1:20, respectively, in blocking buffer overnight. After washing with phosphate-buffered saline, the primary antibody was detected using an avidin–biotin complex immunoperoxidase technique (Zymed Laboratories, Inc., Carlsbad, CA). No staining was observed when the primary antibody was substituted with mouse isotype control.

Liver Section, Enrichment of Nodular Tissue, and Tumor Dissection

Hepatocellular tumors with diameters larger than 5 mm were easily dissected, and their corresponding nontumorous (Nt) liver tissues were obtained. Small nodular lesions 0.5 to 3 mm in diameter were distinguished by their sharp grayish white color demarcation from the surrounding reddish brown liver. Then a stainless steel cork borer (internal diameter, 1 mm) was introduced into frozen tissues. In this way, between 15 and 25 nodules per liver were collected, pooled, and stored in RNA*later* at −80°C. These samples were designated as enriched nodular tissues (ENTs). The increased presence of the hepatocarcinogenesis markers GSTP and GGT in ENT was verified by comparative reverse transcription–polymerase chain reaction (RT-PCR).

RNA Isolation, cDNA Synthesis, Labeling, and Purification

The total RNA of normal livers (NL), ENT of 1 month (ENT-1), ENT of 5 months (ENT-5), and individual HCC samples were obtained by tissue homogenization and extraction with Trizol (Life Technologies, Inc.). After DNase treatment, RNA was purified by phenol chloroform extraction. RNA quality and concentration were determined by capillary electrophoresis (RNA Nano LabChip; Agilent Technologies, Massy, France). For cDNA synthesis, 20 μg of RNA was reverse-transcribed for 1.5 hours at 42°C with 200 U of Superscript II reverse transcriptase (Invitrogen, Carlsbad, CA); 6 μl of 5× first strand buffer (Invitrogen); 1 μg of oligo(dT_{15}); 50 μCi of [α-^{33}P]dCTP (2500 Ci/mmol; Amersham Biosciences, Pittsburgh, PA); 5 μM dCTP; 0.8 mM each of dATP, dGTP, and dTTP; and 10 mM dithiothreitol, in a final volume of 30 μl. After 1 hour, 200 U of Superscript II reverse transcriptase was added to the reaction mixture. The resulting ^{33}P-labeled cDNA was purified with MicroSpin S-200 HR columns (Amersham Biosciences), according to the manufacturer's instructions.

cDNA Microarray Membrane and Hybridization

Atlas rat toxicology cDNA expression 1.2 arrays (7860-1) were purchased from Clontech Laboratories, Inc. (Palto Alto, CA) The membranes contained 1176 known rat genes and 9 housekeeping control cDNA. The arrays were prehybridized with 15 ml of Church buffer [18] and 0.5 mg of denatured salmon testes DNA at 65°C for 2 hours, with continuous agitation. Then, ^{33}P-labeled cDNA was added to the hybridization buffer at 65°C overnight. The membranes were washed at 65°C with 40 mM sodium phosphate buffer (pH 7.2) and 0.1% sodium dodecyl sulfate.

Imaging and Analysis

The membranes were then exposed to low-energy phosphorimage screens for 2 days. Images were acquired with a PhosphorImager 445 SI (Molecular Dynamics/Amersham Biosciences, Pittsburgh, PA). The spots were detected with XDotsReader (v. 1.8), and data were analyzed with the web service BioPlot (http://biopuce.insa-toulouse.fr/; Genopole-Toulouse, Toulouse, France). The intensity of each spot was corrected by subtracting the background; for normalization, the intensity of each spot was divided by the mean intensity of the nine housekeeping genes. From the RNA of rat livers (NL = 3; ENT-1 = 3; ENT-5 = 3; HCC = 3), 12 independent sets of data were obtained. Ratio was obtained from the

average intensity (n = 3) of each gene compared with NL. Statistical data, such as P values from Student's t test and false discovery rate (FDR), were obtained with the BioPlot system. Genes with statistical significance ($P \leq .05$ according to Student's t test) were considered differential genes and were classified as downregulated (< 1) or upregulated (> 1) genes according to the ratio. They were grouped and classified with the web service BioClust (http://biopuce.insa-toulouse.fr/). Two hundred ninety differential genes detected in this study through their statistical values are listed in Table W1. The level of similarity of gene expression patterns was obtained by hierarchical clustering analysis, as determined by Euclidean distance and a complete linkage method using the web-available software Hierarchical Clustering Explorer (http://www.cs.umd.edu/hcil/hce/).

Comparative RT-PCR

RT-PCR was performed by a modification of the comparative PCR method [19]. Both cDNA synthesis and PCR were performed in one step (One Step RT-PCR System; Gibco Invitrogen Corp., Carlsbad, CA). Appropriate primers (0.2 μM each) and 1 μg of total RNA per 50 μl of reaction were used. The absence of DNA contamination was verified by PCR assay. Cycling parameters were as follows: 30 minutes at 45°C for cDNA synthesis, followed by 1 minute at 94°C; annealing for 45 seconds between 52°C and 60°C, followed by 1 minute at 72°C; and final elongation for 10 minutes at 72°C. An adequate number of cycles corresponding to exponential amplification was performed to avoid saturated products with a kinetic analysis of 20–35 cycles for each gene. Primer set sequences are shown in Table 1.

Results

Progression Stage in the Modified RH Model

Hepatocyte nodules and tumor lesions were identified by determination of the marker GGT and by H&E staining (Figure 1). The amount of liver lesions expressing positive GGT activity during the progression stage is shown in Table 2. Numerous nodules up to 2 mm in diameter were uniformly stained for GGT activity at 1 month (Figure 1*A*). They contained clear eosinophilic cytoplasmic hepatocytes with minimal nuclear atypia (Figure 1*B*). The number of nodules showed a significant decrease from 1 to 5 months (Table 2), which is associated with the presence of remodeling and persistent nodules, as described by Enomoto and Farber [20]. Persistent nodules were detected mainly at 5 months, and they showed the largest areas (up to 3 mm^2) with a uniform presence of GGT activity (Figure 1*C*). They had cytologic features similar to those of early nodules, but the increased size of the lesion compressed the surrounding NL (Figure 1*D*). HCC were found after 7 months, and with higher incidence at 12 months (Table 2). These lesions with variable histologic GGT activity had areas greater than 5 mm^2 (Figure 1*E*). HCC exhibited increased thickness of the layers of hepatocytes, marked nucleoli, mitotic figures, nuclear atypia, and anisonucleosis (Figure 1*F*).

Identification of Genes with Differential Expression in Hepatocellular Lesions

To investigate genes related to the progress of nodules toward HCC, the gene expression profiles of liver lesions samples (n = 3) were compared to NL profiles. The number of differential genes between ENT-1/NL, ENT-5/NL, and HCC/NL was 143, 172, and 156, respectively, corresponding to 290 genes. Venn diagram (Figure 2) was used to classify the 290 genes whose expression change was specific to or common in the comparisons. The complete data, including Venn diagram sections, gene names, functional classifications, ratios, and FDRs, are shown in Table W1. According to the main functions of the differential genes in Table W2, the highest proportion of selected genes was related to cellular metabolism (80 genes), followed by cell receptors and intracellular transducer genes (31 and 30 genes, respectively).

Differential genes with intersections between ENT and HCC were considered important because they could reflect the continuous process from preneoplasia to neoplasia. From

Table 1. Primer Pairs Used for RT-PCR in This Study.

Gene Name	Short Name	GenBank Accession Number	Forward and Reverse Primers (5′–3′)	Product Size (bp)
Glutathione *S*-transferase pi 1	*GSTP1*	X02904	TGCCACCGTACACCATTGTGT; CAGCAGGTCCAGCAAGTTGTA	479
Glutamate–cysteine ligase, catalytic subunit	*GCLC*	J05181	GCTGCATCGCCATTTTACCGAG; TGGCAACAGTCATTAGTTCTCCA	883
Glutamate cysteine ligase, modifier subunit	*GCLM*	L22191	AGCTGGACTCTGTCATCATGG; TGGGTCATTGTGAGTCAGTAGC	290
Glutathione synthetase	*GSS*	L38615	CACTATCTCTGCCAGCTTTGG; GTTCCTTTCCTTCTCCTGAGC	211
Annexin 5	*ANXA5*	M21730	ATGGCTCTCAGAGGCACCGT; CGTGTTTCAGCTCGTAGGCG	289
Glutathione reductase	*GSR*	U73174	CCATGTGGTTACTGCACTTCC; TTCTGGAACTCGTCCACTAGG	171
γ-Glutamyl transpeptidase	*GGT1*	M33821	CTCTGCATCTGGCTACCCAC; GGATGCTGGGTTGGAAGAGG	418
Cytochrome *P*450, subfamily IIC (CYP2C11)	*CYP2C11*	J02657	TCATTCCCAAGGGTACCAATG; GGAACAGATGACTCTGAATTCT	664
Sulfotransferase, estrogen-preferring	*STE*	M86758	CTGGAGAGAGACCCATCAGC; TCATTTGCTGCTGGTAGTGC	223
Betaine–homocysteine methyltransferase	*BHMT*	AF038870	GTCATGCAGACCTTCAC*T*TTCTA; TAAGGCCTCGACTGCCCACACG	315
Regucalcin	*RGN*	D38467	AGATGAACAAATCCCAGAT; ACCCTGCATAGGAATATGG	305
α-Actin	α-*ACTIN*	X80130	CCAAGGCCAACCGCGAGAAGATGAC; AGGGTACATGGTGGTGCCGCCAGAC	584

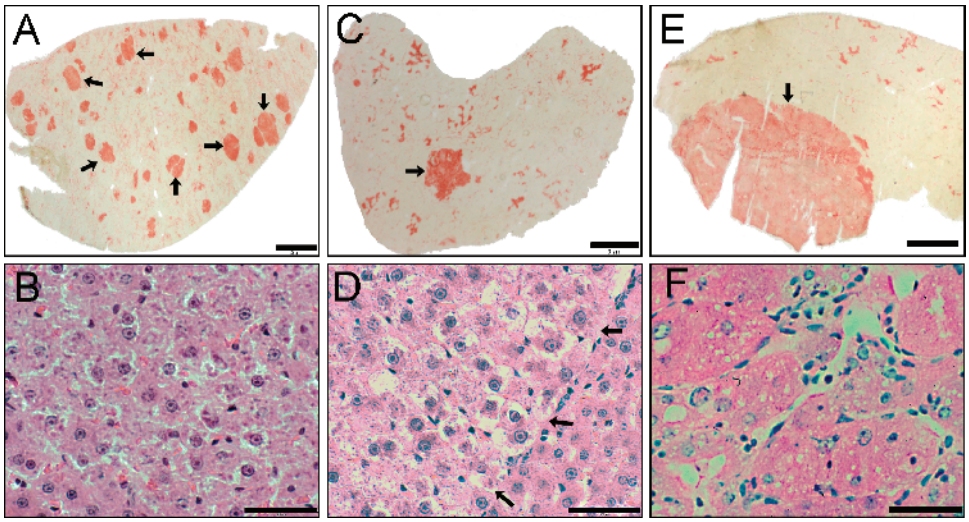

Figure 1. *Progression of hepatocyte nodules toward HCC in the modified RH model. Histologic determination of GGT activity in early nodules (arrows) of 1 month (A), intermediate persistent nodule (arrow) of 5 months (C), and HCC (arrow) of 12 months (E). The increased cytologic alterations and distorted hepatocyte rearrangement in the liver were visualized by H&E staining in an early nodule (B), in a persistent nodule (arrows indicate the borderline of a nodule) (D), and in HCC (F). Bars in (A), (C), and (E) correspond to 2 mm, whereas bars in (B), (D), and (F) correspond to 50 μm.*

the intersection of genes among the three comparisons, 72 genes shared between ENT and HCC were selected; 40 of these showed statistical significance in the three lesion development stages. These genes are displayed in Figure 3 according to ratio; their classification by hierarchical clustering indicates the different patterns of gene expression from early nodules to HCC. Analysis of clustered data revealed at least five behaviors in gene expression patterns. There are upregulated genes in clusters 1 and 2; the first cluster includes upregulated genes with a high ratio in three lesion development stages, such as the known hepatocarcinogenesis marker GST pi with ratios of ENT-1/NL = 13.59, ENT-5/NL = 21.89, and HCC/NL = 22.76, whereas upregulated genes in cluster 2 showed a high ratio in two lesion development stages (e.g., glutamate–cysteine ligase modifier; ENT-1/NL = 1.26, ENT-5/NL = 2.42, and HCC/NL = 4.59). Cluster 3 includes genes with transitions from upregulated levels in ENT to downregulated levels in HCC (e.g., metallothionein; ENT-1/NL = 5.08, ENT-5/NL = 2.29, and HCC/NL = 0.55). Cluster 4 includes genes with transitions from downregulated levels in ENT-1 to upregulated levels in HCC (e.g., cyclin D1; ENT-1/NL = 0.34, ENT-5/NL = 0.41, and HCC/NL = 2). Cluster 5 contains downregulated genes in three lesion development stages (e.g., CYP450-2C11; ENT-1/NL = 0.37, ENT-5/NL = 0.34, and HCC/NL = 0.14).

To extend the selection of important differential genes in hepatocarcinogenesis, from the 84 genes that showed statistical significance only in HCC, the highly upregulated genes (ratio ≥ 2) and the highly downregulated genes (ratio ≤ 0.5) were selected; the expression level of these 35 genes in the three lesion development stages is shown in Figure 4. Clustering analysis resulted in four gene clusters: cluster 1, highly upregulated genes in HCC with a tendency for upregulation in ENT (e.g., Annexin 5; ENT-1/NL = 1.39, ENT-5/NL = 1.43, and HCC/NL = 3.63); cluster 2, highly upregulated

Table 2. Quantitative Histologic Analysis of GGT-Positive Hepatocellular Lesions in Rats.

Sacrifice (months)	Nodules/cm^2 (Mean ± SD)	Persistent Nodules (%)*	Rats with HCC
1	22.31 ± 3.74	1.85 ± 1.7	0/7
3	15.25 ± 1.80	3.89 ± 2.6	0/3
5	4.71† ± 1.77	14.61† ± 7.2	0/6
7	16.06 ± 7.34	1.99 ± 3.4	2/4
12			6/6

*Uniformly stained nodules with area > 1 mm^2.
†Statistically different compared with the 1-month group.

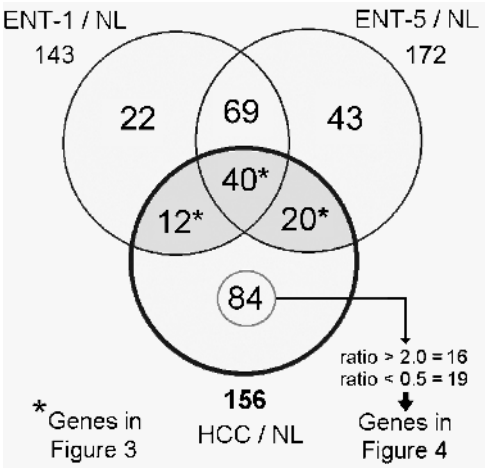

Figure 2. *Differentially expressed genes in liver lesions against NL. Venn diagram of 290 differential genes. Considering NL as reference, the differential genes were determined by statistical significance (P ≤ .05, Student's t test) in ENT-1, ENT-5, and HCC samples (n = 3 for each sample). From the intersection (*), 72 genes that were shared by ENT-1, ENT-5, and HCC are listed in Figure 3. From the 84 differential genes in HCC/NL, 19 highly downregulated (ratio ≤ 0.5) and 16 highly upregulated (ratio ≥ 2) genes are listed in Figure 4.*

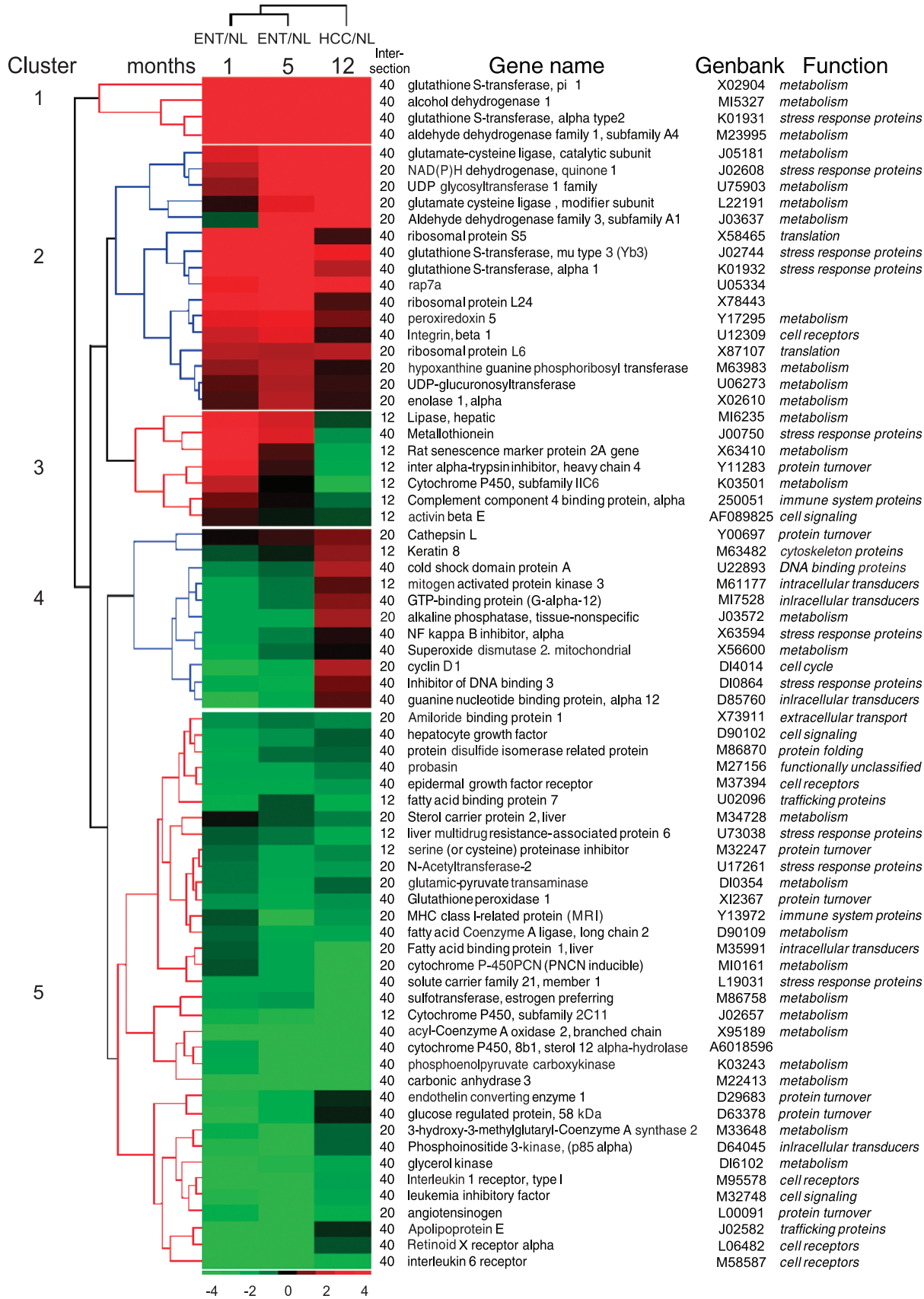

Figure 3. *Gene expression patterns of 72 genes shared by ENT and HCC. As indicated in Figure 2, the genes from intersections 12*, 40*, and 20* were compiled. The labels of intersection in the Venn diagram, gene names, GenBank accession numbers, and main functions are shown. The genes were classified by hierarchical clustering, and the ratio average of each type of sample (columns) is presented in a matrix format. Green and red represent downregulation and upregulation, respectively, as indicated in the scale bar (log_2 ratio–transformed scale). The dendrogram in blue or red on the left indicates the degree of similarity of selected genes. The clusters indicate the different behaviors of genes in the three types of sample.*

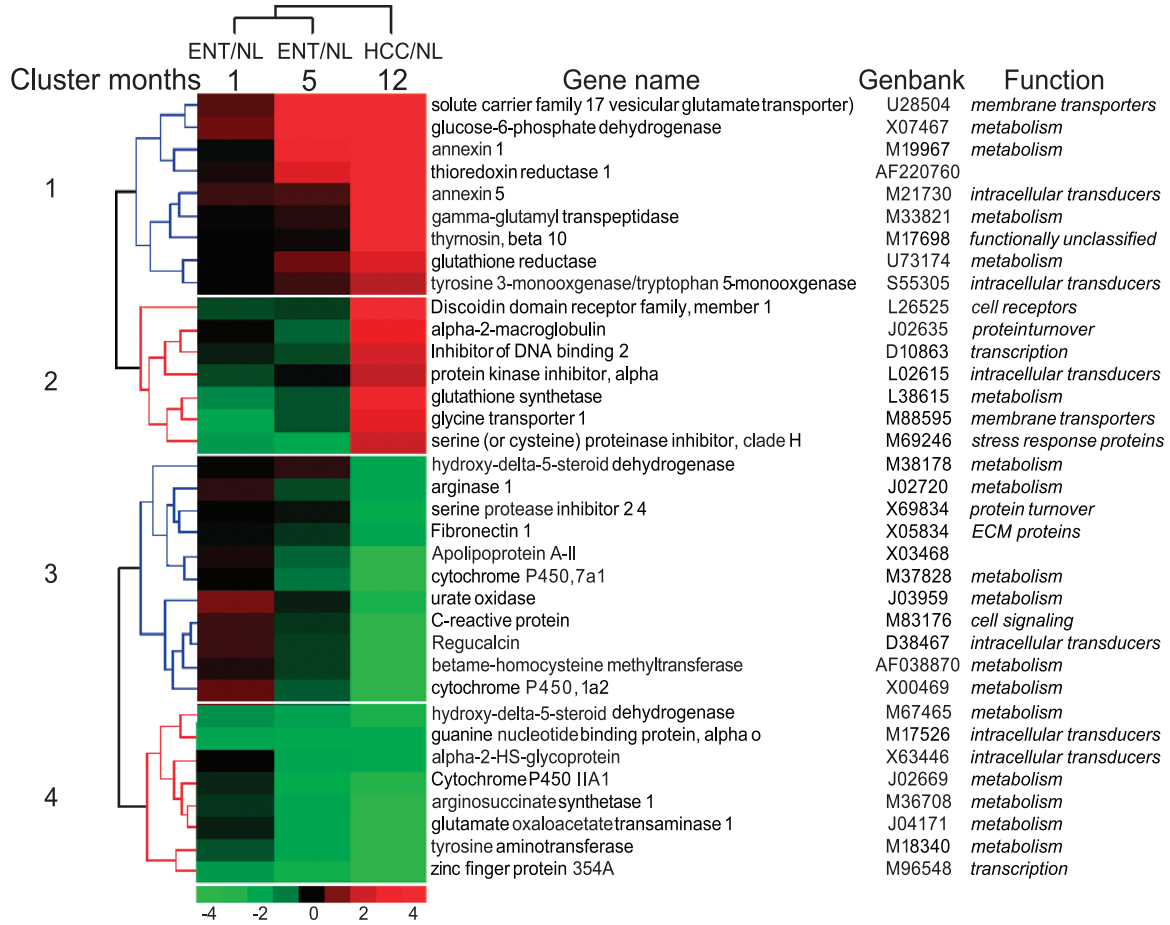

Figure 4. *Gene expression patterns of highly upregulated or downregulated genes in HCC. As indicated in Figure 2, genes with an expression ratio that had at least a two-fold difference were selected from the 84 genes that showed a statistical difference ($P \leq .05$) only in the HCC/NL comparison. The genes were classified by hierarchical clustering as in Figure 3.*

genes in HCC with a tendency for downregulation in ENT (e.g., protein kinase inhibitor α; ENT-1/NL = 0.72, ENT-5/NL = 0.94, and HCC/NL = 2.08); cluster 3, highly downregulated genes in HCC with a tendency for upregulation in ENT [e.g., betaine–homocysteine methyltransferase (BHMT); ENT-1/NL = 1.19, ENT-5/NL = 0.75, and HCC/NL = 0.28]; and, cluster 4, highly downregulated genes in HCC with a tendency for downregulation in ENT (e.g., cytochrome *P*450 IIA1; ENT-1/NL = 0.83, ENT-5/NL = 0.39, and HCC/NL = 0.34).

Immunohistologic Analysis of GSTP and Cyclin D1 in HCC

From the upregulated genes in HCC (Figure 3), the highest ratio (HCC/NL = 23) was found for the *GSTP* gene, which is the most important marker in rat hepatocarcinogenesis models; at the limits, the gene that is considered highly upregulated (HCC/NL = 2) is *cyclin D1*, which is an important oncogene involved in cell cycle regulation. To confirm the upregulation of these genes at the protein level, immunohistochemistry was performed in histologic serial sections of HCC (Figure 5). A specific increased level of GSTP in the cytoplasm of HCC cells was evident when compared to adjacent tissues (Figure 5*A*). In the same way, cyclin D1 was significantly increased in the nucleus of neoplastic hepatocytes (Figure 5*B*). These genes illustrate that upregulation for some genes at the mRNA level induces increased protein levels.

Comparative RT-PCR Confirming Differential Gene Expression of Selected Genes

To validate cDNA array results, we used comparative RT-PCR for gene expression analysis. From the genes listed in Figures 3 and 4, four downregulated and seven upregulated selected genes (Table 1) were compared with mRNA levels in NL, ENT-1, ENT-5, HCC, and in the corresponding Nt tissues of two rats sacrificed at 15 months (Figure 6). There was a notable correspondence in the ratios obtained from cDNA arrays and the band level determined by RT-PCR. The 11 genes analyzed were consistent with their respective downregulation or upregulation in ENT and HCC with respect to NL. Because the surrounding Nt tissue is an important reference for histologic demarcation of tumor and marker discovery, we compared mRNA levels between these two samples. It is significant to note that there were higher levels of upregulated genes in tumors than in Nt tissues, and vice versa in downregulated genes. Thus, besides the validation of the altered expression of these genes, they could be

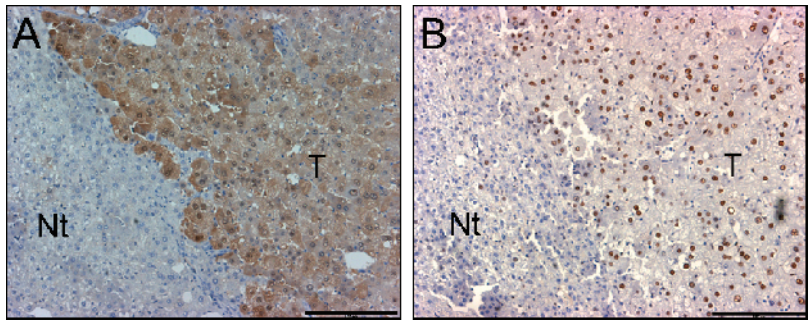

Figure 5. *Histologic confirmation of increased GSTP and cyclin D1 levels in HCC. Immunoperoxidase staining of GSTP (A) and cyclin D1 (B) in serial sections of HCC of a rat sacrificed 15 months after initiation. Scale bars, 200 μm.*

important for the histologic distinction of tumors from adjacent Nt tissues.

Discussion

Animal models of hepatocarcinogenesis recapitulate the underlying biology of liver tumorigenesis and have provided reliable data for understanding the cellular development of HCC in humans [21–23]. The progression stage in the RH model is characterized by the evolution from nodules to HCC without additional carcinogen treatment. The majority of nodules remodel or differentiate into a liver of normal appearance, whereas a few persistent nodules show spontaneous cell proliferation and size increase [20,24–26]. Considering that all rats with hepatic nodular lesions will present with HCC after 9 to 10 months [11], it is possible to hypothesize that nodular cells may have an altered genetic background that allows them to accumulate additional mutations and, after a selection process, to show autonomous cell proliferation. These genetic alterations should predispose nodules to undergoing a slow evolution to cancer; however, this issue remains unclear.

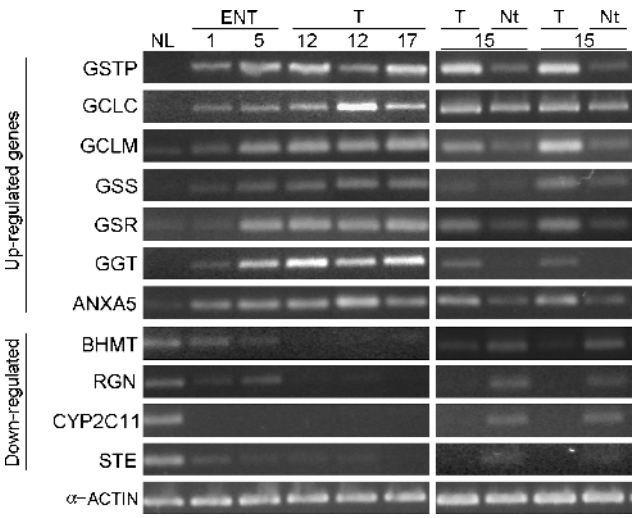

Figure 6. *Confirmation of the differential expression of 11 genes by RT-PCR. Comparison of mRNA levels of 11 selected genes plus α-actin as control in NL, ENT-1, and ENT-5; individual tumors (T) at 12 and 17 months; and pairs of tumors (T) and corresponding Nt tissues at 15 months. Only for RT-PCR were RNA samples of NL and ENT pooled from three livers. Full gene names are shown in Table 1.*

One positive feature of this model is its ability to distinguish a few persistent nodules from a large number of remodeling nodules and, thus, to allow a study of the nodule's cancer sequence [11]. According to our histologic analysis, the highest proportion of persistent nodules without HCC occurrence was found at 5 months. Although they were few in the liver, the increase in size of up to 3 mm in diameter allowed us to collect them easily from the frozen liver. Thus, we performed the study at three periods of progression: initial point, with tissues that included early nodules (1 month); intermediate point, with tissues that included persistent nodules (5 months); and end point, with well-developed HCC (12 months).

The evaluation of array results against NL, together with statistical analysis, allowed us to reveal differential gene expression patterns within each progression condition and to compare them. The known hepatocarcinogenesis markers such as α_2-*macroglobulin* [27], *GGT*, and *GSTP* were upregulated, showing congruence of cDNA array results. With equal coherence, the oncogene *cyclin D1* showed a two-fold increased mRNA level in array results and an increased protein presence in GSTP-positive cancer cells. Furthermore, differential gene expression was validated for 11 genes by comparative RT-PCR (four downregulated genes and seven upregulated genes). It is important to note that the expression of these genes was also compared in tumorous and corresponding adjacent Nt tissues of two rats sacrificed 15 months after DEN treatment, showing that tumorous tissues can be molecularly differentiable from surrounding tissues. The differential mRNA levels of the indicated genes in tumor and nontumor tissues could be useful for the development of additional tools for the histopathological evaluation and confirmation of HCC. There is a need for a noninvasive method for early HCC diagnosis; for this reason, we will perform additional studies focusing on gene products such as the secreted protein Annexin 5, which will lead to the identification of serological markers.

It is known that hepatocyte nodules are precursors for HCC [26]. With this in mind, we selected the genes that were statistically significant from preneoplasia to neoplasia; these

72 genes showed a wide pattern of expression courses from tissues with early nodules to liver cancer. Those genes with consistent upregulation (i.e., *GCL*, glutamate–cysteine ligase, and others) or with consistent downregulation (i.e., *sulfotransferase*, *estrogen-preferring*; *CYP2C11*; and others) from early nodules to HCC may form a fraction of an altered gene expression environment that predisposes nodules to progressing into HCC, and they would be considered as underlying genes involved in the progression stage of hepatocarcinogenesis. It was not surprising that, among these genes, *GSTP* was found because it is widely used as a marker in the basic analysis of chemical carcinogenesis [28,29]. Furthermore, other *GST* gene family members (i.e., α and μ) were upregulated with a similar course of expression, indicating perhaps the same transcriptional regulation or response to inducers [30].

The systems of transforming growth factor α and hepatocyte growth factor (HGF), and their receptors epidermal growth factor receptor (EGFR) and *met* proto-oncogene, respectively, are mitogenic for hepatocytes and have been suggested to contribute to HCC formation [31,32]. In our results, the four genes showed downregulated levels from early nodules to HCC, with ratios between 0.34 and 0.67 (Table W1). Our data are in agreement with previous reports that showed no increased presence of these gene products in rat preneoplastic and neoplastic hepatocytes [31,33,34]. In human HCC, expression of HGF and EGFR has shown great variability with respect to the pattern of histologic differentiation of HCC [35,36]. However, other growth factors showed upregulation in at least one lesion development stage, as follows (ENT-1, ENT-5, and HCC): *fibroblast growth factor 10*—4.09, 4.24, and 1.37; *insulin-like growth factor 1*—2.53, 1.3, and 0.48; insulin-like growth factor binding protein 1 (*Igfbp1*)—2.46, 2.5, and 1.1; and Igfbp3—0.4, 0.6, and 2.07 (Table W1). The results from these growth factor studies have stimulated us to undertake additional investigations to understand the preferential cell proliferation of preneoplastic and neoplastic lesions.

There is strong evidence for the involvement of oxidative stress in hepatocarcinogenesis. Oxidative stress may trigger damage to cellular membranes and nuclear DNA, which result in lipid peroxidation and oxidative DNA damage, respectively. Here, by statistical selection, we have detected several differential genes involved in the control and regulation of oxidative stress: upregulated genes such as those for *NAD(P)H dehydrogenase quinone* 1, *superoxide dismutase* 2, *mitochondrial alcohol dehydrogenase* 1, *peroxiredoxin*, and *thioredoxin reductase* 1; downregulated genes such as those for *carbonic anhydrase* 3 and *glutathione peroxidase*; and genes with a transition from upregulated levels in preneoplasia to downregulated levels in cancer, such as that for *metallothionein*. The specific increase at the protein level of metallothionein in rat liver preneoplastic lesion has been demonstrated by Sawaki et al. [37], whereas downregulated expression in hepatocellular tumors has been described for human and mouse chemical carcinogenesis [38]. Although the participation of metallothionein in cell proliferation and carcinogenesis has been suggested [39], additional analysis should be performed to examine the possible correlation between its expression and preneoplastic/neoplastic transition.

Many reports indicate that reduced glutathione (GSH) and its cooperating enzymes are important in neoplastic diseases and play a crucial role in defense against reactive oxygen species [40,41]. In rat chemical hepatocarcinogenesis models, increased levels of GSH, oxidized glutathione, GGT, and GSTP are often detected in preneoplastic hepatocyte nodules and hepatocellular tumors [42,43]. In our transcriptome analysis, we detected more than 10 genes that are involved in GSH metabolism. Figure 7 maps the modulation of some differential genes at mRNA levels in HCC in the metabolic pathways of GSH biosynthesis, amino acid recycling, antioxidation in GSH, and redox control for DNA synthesis. The upregulation of the *GCLC*, *GCLM*, and *GSH synthetases* essential for GSH biosynthesis could explain the increased levels of total glutathione in hepatocarcinogenesis. Moreover, the upregulation of *GGT*, glycine transporter 1 (*Slc6a9*), and solute carrier family 17-vesicular glutamate transporter member 1 (*Slc17a1*) could favor the catabolism of extracellular GSH and the recovery of glycine and glutamate, respectively. The downregulation of the liver multidrug resistance–associated protein 6 gene (*Abcc6*), which acts as a MgATP-dependent efflux pump that transports glutathione *S*-conjugates [44], could maintain the increased level of intracellular glutathione. One of the major determinants of the rate of GSH synthesis is the availability of cysteine [45]; *N*-acetyltransferase-2 catalyzes the *N*-acetylation of the cysteine conjugate (X-Cys), resulting in the formation of mercapturic acid, which is usually excreted in urine (its downregulated expression in hepatocellular tumors could be an adaptive response to maintaining the amount of cysteine essential for GSH biosynthesis). Another important source of cysteine comes from the trans-sulfuration pathway, which converts methionine to cysteine. Methionine can be resynthesized from homocysteine through the activity of BHMT; this gene was downregulated in tumors, favoring the idea that maintaining cysteine for GSH biosynthesis is an adaptive response of neoplastic cells.

GST gene products and GSH peroxidase 1 (Gpx1) share the ability to reduce organic peroxides through GSH oxidation. Nevertheless, contrary to *GST* genes, the *Gpx1* gene was downregulated from early nodules to HCC, indicating that liver cancer may develop in a *Gpx1*-deficient condition. Reduced expression of this gene was reported in rat experimental HCC [46], and reduced activity was reported in human HCC [47,48]. The reduction of this important scavenger enzyme of toxic oxygen radicals exemplifies a shared phenomenon in HCC development in humans and rats.

Several reports and our data suggest that the altered gene expression of oxidative stress–related genes and GSH metabolism genes plays an important role in predisposing nodular hepatocytes to progression toward HCC. GSH level increases in human HCC and hepatocytes during active proliferation with respect to NL [45,49]. An increased level of GSH has been detected in a number of drug-resistant tumor cell lines and in tumor cells isolated from patients

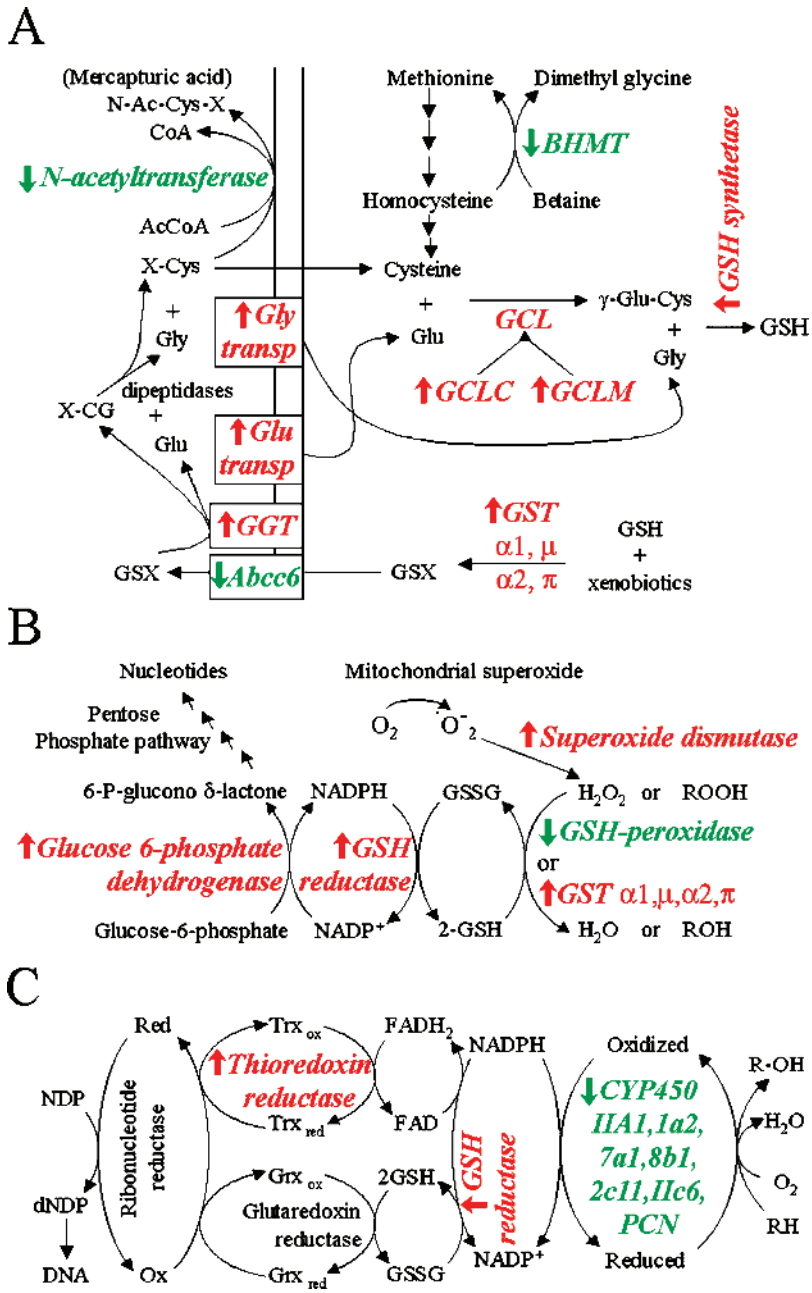

Figure 7. *Mapping of some differentiable genes in cellular metabolic pathways. (A) Glutathione (GSH) biosynthesis and amino acid recycling. (B) Antioxidant function of GSH. (C) Role of GSH and NADPH in DNA synthesis and cytochrome oxidation. (↑) Upregulated differential genes (red). (↓) Downregulated differential genes (green). BHMT, betaine–homocysteine methyltransferase; GGT, γ-glutamyl transpeptidase; GCL, glutamate cysteine ligase; GST, glutathione S-transferase; Abcc6, liver multidrug resistance-associated protein 6.*

whose tumors are clinically resistant to drug therapy [50]. In human HCC, increased hepatic oxidative DNA damage has been reported on patients with HCC [51,52]. However, in the future, it will be important to determine the chronological causative participation of oxidative stress and GSH regulation in human and rat hepatocarcinogeneses.

Gene expression profiles provide a guide for the understanding of HCC development. Hierarchical clustering classification also allowed us to conclude that the pattern of gene expression is more similar between nodular samples at 1 and 5 months relative to HCC. A similar concept was found histologically in H&E staining (Figure 1), in which the cytologic features of early and persistent nodular hepatocytes are modestly altered with respect to neoplastic cells in cancer. Thus, gene profiles exemplify the continuous progression from nodules to HCC.

Numerous researchers have used microarrays to profile the gene expression pattern of human HCC, and they have found thousands of altered genes [15,22,27,53]. However, among these genes, it is difficult to discern which are critical for HCC development and are not just a consequence of increased genomic instability. It is known that liver cancer, as with other solid malignancies, displays a high number of genetic alterations and huge heterogeneity in gene expres-

sion profiles. For this reason, it is essential to differentiate the important genes implicated in liver tumorigenesis with respect to those genes that are not related to cancer development or are considered as biologic noise.

The gene expression patterns associated with human HCC progression have been addressed by a comparison of early HCC and nodule-in-nodule-type HCC (advanced HCC within early HCC) [53]. Heat shock protein 70 (HSP70) was identified as a marker of early HCC. Coincidentally, we found increased levels of the *HSP70-8* in ENT-1 (ratio = 2.79), ENT-5 (ratio = 2.99), and HCC (ratio = 1.51) (Table W1). Lee et al. [22] have revealed two subclasses of HCC patients, characterized by the expression profiles of a limited number of genes that accurately predict the length of survival. Some of these genes with downregulated levels [such as regucalcin (*RGN*), insulin receptor (*Insr*), interleukin 6 receptor (*Il6r*), enoyl coenzyme A hydratase short chain 1 (*Echs1*), androgen receptor (*Ar*), and acyl coenzyme A oxidase 2 branched chain (*Acox2*)] were also downregulated in rat HCC (Table W1), whereas upregulated genes [such as tyrosine 3-monooxygenase/tryptophan 5-monooxygenase activation protein eta polypeptide (*Ywhah*); serine (or cysteine) proteinase inhibitor clade H, member 1 (*Serpinh1*); ribosomal proteins S3, S5, and S9 (*Rps3*, *Rps5*, and *Rps9*); nucleophosmin 1 (*Npm1*); fatty acid binding protein 5 epidermal (*Fabp5*); and cold shock domain protein A (*Csda*)] were increased in both human and rat HCC. The potential of the RH model, together with DNA microarray technology, has allowed us to reveal gene expression changes in rat HCC that could be relevant to human HCC.

To increase the screening of global gene expression during hepatocarcinogenesis, we are now expanding our study to high-density oligonucleotide microarrays. In the present work studying 1185 rat genes, it was possible to identify a gene expression profile that is related to the progression of rat hepatocarcinogenesis, which suggests altered cellular homeostasis as a predisposing factor for the evolution of nodules toward cancer. Furthermore, data may provide opportunities to find new markers for rat liver preneoplastic nodules and target genes for chemoprevention or early treatment of HCC.

Acknowledgements

We are grateful to J. Fernandez, M. Flores, R. Leyva, and R. Gaxiola for technical support at the Animal House.

References

[1] Plentz RR, Tillmann HL, Kubicka S, Bleck JS, Gebel M, Manns MP, and Rudolph KL (2005). Hepatocellular carcinoma and octreotide: treatment results in prospectively assigned patients with advanced tumor and cirrhosis stage. *J Gastroenterol Hepatol* **20,** 1422–1428.

[2] Okuda K (1992). Hepatocellular carcinoma: recent progress. *Hepatology* **15,** 948–963.

[3] Hussain SM, Zondervan PE, I. Jzermans JN, Schalm SW, de Man RA, and Krestin GP (2002). Benign *versus* malignant hepatic nodules: MR imaging findings with pathologic correlation. *Radiographics* **22,** 1023–1036 (discussion, 1037–1029).

[4] Saffroy R, Pham P, Lemoine A, and Debuire B (2004). Molecular biology and hepatocellular carcinoma: current status and future prospects. *Ann Biol Clin (Paris)* **62,** 649–656.

[5] Choi BI (2004). The current status of imaging diagnosis of hepatocellular carcinoma. *Liver Transpl* **10,** S20–S25.

[6] Carrasco-Legleu CE, Marquez-Rosado L, Fattel-Fazenda S, Arce-Popoca E, Perez-Carreon JI, and Villa-Trevino S (2004). Chemoprotective effect of caffeic acid phenethyl ester on promotion in a medium-term rat hepatocarcinogenesis assay. *Int J Cancer* **108,** 488–492.

[7] Marquez-Rosado L, Trejo-Solis MC, Garcia-Cuellar CM, and Villa-Trevino S (2005). Celecoxib, a cyclooxygenase-2 inhibitor, prevents induction of liver preneoplastic lesions in rats. *J Hepatol* **43,** 653–660.

[8] Yamamoto T, Kaneda K, Hirohashi K, Kinoshita H, and Sakurai M (1996). Sinusoidal capillarization and arterial blood supply continuously proceed with the advance of the stages of hepatocarcinogenesis in the rat. *Jpn J Cancer Res* **87,** 442–450.

[9] Pascale RM, Simile MM, De Miglio MR, Muroni MR, Calvisi DF, Asara G, Casabona D, Frau M, Seddaiu MA, and Feo F (2002). Cell cycle deregulation in liver lesions of rats with and without genetic predisposition to hepatocarcinogenesis. *Hepatology* **35,** 1341–1350.

[10] Solt D and Farber E (1976). New principle for the analysis of chemical carcinogenesis. *Nature* **263,** 701–703.

[11] Farber E and Sarma DS (1987). Hepatocarcinogenesis: a dynamic cellular perspective. *Lab Invest* **56,** 4–22.

[12] Solt DB, Cayama E, Tsuda H, Enomoto K, Lee G, and Farber E (1983). Promotion of liver cancer development by brief exposure to dietary 2-acetylaminofluorene plus partial hepatectomy or carbon tetrachloride. *Cancer Res* **43,** 188–191.

[13] Rotstein J, Macdonald PD, Rabes HM, and Farber E (1984). Cell cycle kinetics of rat hepatocytes in early putative preneoplastic lesions in hepatocarcinogenesis. *Cancer Res* **44,** 2913–2917.

[14] Kim JW and Wang XW (2003). Gene expression profiling of preneoplastic liver disease and liver cancer: a new era for improved early detection and treatment of these deadly diseases? *Carcinogenesis* **24,** 363–369.

[15] Zhang LH and Ji JF (2005). Molecular profiling of hepatocellular carcinomas by cDNA microarray. *World J Gastroenterol* **11,** 463–468.

[16] Sanchez-Perez Y, Carrasco-Legleu C, Garcia-Cuellar C, Perez-Carreon J, Hernandez-Garcia S, Salcido-Neyoy M, Aleman-Lazarini L, and Villa-Trevino S (2005). Oxidative stress in carcinogenesis. Correlation between lipid peroxidation and induction of preneoplastic lesions in rat hepatocarcinogenesis. *Cancer Lett* **217,** 25–32.

[17] Rutenburg AM, Kim H, Fischbein JW, Hanker JS, Wasserkrug HL, and Seligman AM (1969). Histochemical and ultrastructural demonstration of gamma-glutamyl transpeptidase activity. *J Histochem Cytochem* **17,** 517–526.

[18] Church GM and Gilbert W (1984). Genomic sequencing. *Proc Natl Acad Sci USA* **81,** 1991–1995.

[19] Brass N, Heckel D, and Meese E (1998). Comparative PCR: an improved method to detect gene amplification. *Biotechniques* **24,** 22–24, 26.

[20] Enomoto K and Farber E (1982). Kinetics of phenotypic maturation of remodeling of hyperplastic nodules during liver carcinogenesis. *Cancer Res* **42,** 2330–2335.

[21] Thorgeirsson SS and Grisham JW (2002). Molecular pathogenesis of human hepatocellular carcinoma. *Nat Genet* **31,** 339–346.

[22] Lee JS, Chu IS, Heo J, Calvisi DF, Sun Z, Roskams T, Durnez A., Demetris AJ, and Thorgeirsson SS (2004). Classification and prediction of survival in hepatocellular carcinoma by gene expression profiling. *Hepatology* **40,** 667–676.

[23] Feitelson MA, Pan J, and Lian Z (2004). Early molecular and genetic determinants of primary liver malignancy. *Surg Clin North Am* **84,** 339–354.

[24] Tatematsu M, Nagamine Y, and Farber E (1983). Redifferentiation as a basis for remodeling of carcinogen-induced hepatocyte nodules to normal appearing liver. *Cancer Res* **43,** 5049–5058.

[25] Farber E (1984). Pre-cancerous steps in carcinogenesis. Their physiological adaptive nature. *Biochim Biophys Acta* **738,** 171–180.

[26] Farber E (1987). Experimental induction of hepatocellular carcinoma as a paradigm for carcinogenesis. *Clin Physiol Biochem* **5,** 152–159.

[27] Sukata T, Uwagawa S, Ozaki K, Sumida K, Kikuchi K, Kushida M, Saito K, Morimura K, Oeda K, Okuno Y, et al. (2004). alpha(2)-Macroglobulin: a novel cytochemical marker characterizing preneoplastic and neoplastic rat liver lesions negative for hitherto established cytochemical markers. *Am J Pathol* **165,** 1479–1488.

[28] Hendrich S, Campbell HA, and Pitot HC (1987). Quantitative stereological evaluation of four histochemical markers of altered foci in multistage hepatocarcinogenesis in the rat. *Carcinogenesis* **8,** 1245–1250.
[29] Higashi K, Hiai H, Higashi T, and Muramatsu M (2004). Regulatory mechanism of glutathione *S*-transferase P-form during chemical hepatocarcinogenesis: old wine in a new bottle. *Cancer Lett* **209,** 155–163.
[30] Hayes JD and Pulford DJ (1995). The glutathione *S*-transferase supergene family: regulation of GST and the contribution of the isoenzymes to cancer chemoprotection and drug resistance. *Crit Rev Biochem Mol Biol* **30,** 445–600.
[31] Hu Z, Evarts RP, Fujio K, Omori N, Omori M, Marsden ER, and Thorgeirsson SS (1996). Expression of transforming growth factor alpha/epidermal growth factor receptor, hepatocyte growth factor/c-met and acidic fibroblast growth factor/fibroblast growth factor receptors during hepatocarcinogenesis. *Carcinogenesis* **17,** 931–938.
[32] Schiffer E, Housset C, Cacheux W, Wendum D, Desbois-Mouthon C, Rey C, Clergue F, Poupon R, Barbu V, and Rosmorduc O (2005). Gefitinib, an EGFR inhibitor, prevents hepatocellular carcinoma development in the rat liver with cirrhosis. *Hepatology* **41,** 307–314.
[33] Huitfeldt HS, Skarpen E, Lindeman B, Becher R, Thrane EV, and Schwarze PE (1996). Differential distribution of Met and epidermal growth factor receptor in normal and carcinogen-treated rat liver. *J Histochem Cytochem* **44,** 227–233.
[34] Imai T, Masui T, Nakanishi H, Inada K, Kobayashi K, Nakamura T, and Tatematsu M (1996). Expression of hepatocyte growth factor and c-met mRNAs during rat chemically induced hepatocarcinogenesis. *Carcinogenesis* **17,** 19–24.
[35] D'Errico A, Fiorentino M, Ponzetto A, Daikuhara Y, Tsubouchi H, Brechot C, Scoazec JY, and Grigioni WF (1996). Liver hepatocyte growth factor does not always correlate with hepatocellular proliferation in human liver lesions: its specific receptor c-met does. *Hepatology* **24,** 60–64.
[36] Kira S, Nakanishi T, Suemori S, Kitamoto M, Watanabe Y, and Kajiyama G (1997). Expression of transforming growth factor alpha and epidermal growth factor receptor in human hepatocellular carcinoma. *Liver* **17,** 177–182.
[37] Sawaki M, Enomoto K, Hattori A, Tsuzuki N, Sawada N, and Mori M (1999). Elevation of metallothionein level in preneoplastic lesions during chemical hepatocarcinogenesis of the Fischer 344 rat. *Toxicol Lett* **108,** 55–61.
[38] Waalkes MP, Diwan BA, Rehm S, Ward JM, Moussa M, Cherian MG, and Goyer RA (1996). Down-regulation of metallothionein expression in human and murine hepatocellular tumors: association with the tumor-necrotizing and antineoplastic effects of cadmium in mice. *J Pharmacol Exp Ther* **277,** 1026–1033.
[39] Cherian MG, Howell SB, Imura N, Klaassen CD, Koropatnick J, Lazo JS, and Waalkes MP (1994). Role of metallothionein in carcinogenesis. *Toxicol Appl Pharmacol* **126,** 1–5.
[40] Denda A, Tang Q, Tsujiuchi T, Tsutsumi M, Amanuma T, Murata Y, Tamura K, Horiguchi K, Nakae D, and Konishi Y (1993). Effects of oxidative stress induced by redox-enzyme modulation on the progression stage of rat hepatocarcinogenesis. *Carcinogenesis* **14,** 95–101.
[41] Koike K and Miyoshi H (2005). Oxidative stress and hepatitis C viral infection. *Hepatol Res* **34,** 65–73.
[42] Lu SC, Huang ZZ, Yang H, and Tsukamoto H (1999). Effect of thioacetamide on the hepatic expression of gamma-glutamylcysteine synthetase subunits in the rat. *Toxicol Appl Pharmacol* **159,** 161–168.
[43] Mauriz JL, Linares P, Macias RI, Jorquera F, Honrado E, Olcoz JL, Gonzalez P, and Gonzalez-Gallego J (2003). TNP-470 inhibits oxidative stress, nitric oxide production and nuclear factor kappa B activation in a rat model of hepatocellular carcinoma. *Free Radic Res* **37,** 841–848.
[44] Belinsky MG, Chen ZS, Shchaveleva I, Zeng H, and Kruh GD (2002). Characterization of the drug resistance and transport properties of multidrug resistance protein 6 (MRP6, ABCC6). *Cancer Res* **62,** 6172–6177.
[45] Lu SC (1999). Regulation of hepatic glutathione synthesis: current concepts and controversies. *FASEB J* **13,** 1169–1183.
[46] Lertprasertsuke N, Shinoda M, Takekoshi S, Yoshimura S, and Watanabe K (1990). Suppression of messenger ribonucleic acid for glutathione peroxidase in chemically induced rat hepatocellular carcinoma and its biological significance. *Tokai J Exp Clin Med* **15,** 285–292.
[47] Casaril M, Gabrielli GB, Dusi S, Nicoli N, Bellisola G, and Corrocher R (1985). Decreased activity of liver glutathione peroxidase in human hepatocellular carcinoma. *Eur J Cancer Clin Oncol* **21,** 941–944.
[48] Corrocher R, Casaril M, Bellisola G, Gabrielli G, Hulpe M, Garofoli E, and Nicoli N (1986). Reduction of liver glutathione peroxidase activity and deficiency of serum selenium in patients with hepatocellular carcinoma. *Tumori* **72,** 617–619.
[49] Huang ZZ, Chen C, Zeng Z, Yang H, Oh J, Chen L, and Lu SC (2001). Mechanism and significance of increased glutathione level in human hepatocellular carcinoma and liver regeneration. *FASEB J* **15,** 19–21.
[50] Mulcahy RT, Untawale S, and Gipp JJ (1994). Transcriptional upregulation of gamma-glutamylcysteine synthetase gene expression in melphalan-resistant human prostate carcinoma cells. *Mol Pharmacol* **46,** 909–914.
[51] Schwarz KB, Kew M, Klein A, Abrams RA, Sitzmann J, Jones L, Sharma S, Britton RS, Di Bisceglie AM, and Groopman J (2001). Increased hepatic oxidative DNA damage in patients with hepatocellular carcinoma. *Dig Dis Sci* **46,** 2173–2178.
[52] Jungst C, Cheng B, Gehrke R, Schmitz V, Nischalke HD, Ramakers J, Schramel P, Schirmacher P, Sauerbruch T, and Caselmann WH (2004). Oxidative damage is increased in human liver tissue adjacent to hepatocellular carcinoma. *Hepatology* **39,** 1663–1672.
[53] Chuma M, Sakamoto M, Yamazaki K, Ohta T, Ohki M, Asaka M, and Hirohashi S (2003). Expression profiling in multistage hepatocarcinogenesis: identification of HSP70 as a molecular marker of early hepatocellular carcinoma. *Hepatology* **37,** 198–207.

Table W1. Statistical Differential Genes, Classified According to the Venn's Diagram (Figure 2).

Venn Section	Gene Name	Symbol	Genbank	Functional Classification	Ratio			FDR
					ENT1/NL	ENT5/L	HCC/NL	
12	fatty acid binding protein 7	Fabp7	U02096	trafficking/targeting proteins	0.39*	0.71	0.4*	0.00040
12	liver multidrug resistance-associated protein 6	Abcc6	U73038	stress response proteins	0.68*	0.61	0.42*	0.00050
12	inter alpha-trypsin inhibitor, heavy chain 4	Itih4	Y11283	protein turnover	2.68*	1.35	0.43*	
12	serine (or cysteine) proteinase inhibitor, clade A, member 1		M32247	protein turnover	0.63*	0.48	0.57*	0.00032
12	Lipase, hepatic	Lipc	M16235	metabolism	2.71*	2.25	0.73*	
12	Rat senescence marker protein 2A gene, exons 1 and 2	Smp2a	X63410	metabolism	5.67*	1.44	0.48*	
12	Cytochrome P450, subfamily IIC6	Cyp2c6	K03501	metabolism	2.08*	1.03	0.35*	
12	Cytochrome P450, subfamily IIC (mephenytoin 4-hydroxylase)	Cyp2c	J02657	metabolism	0.37*	0.34	0.14*	0.00049
12	mitogen activated protein kinase 3	Mapk3	M61177	intracellular transducers/ effectors/modulators	0.46*	0.61	1.48*	
12	Complement component 4 binding protein, alpha	C4bpa	Z50051	immune system proteins	1.56*	1.14	0.63*	
12	Keratin 8	Krt2-8	M63482	cytoskeleton/motility proteins	0.69*	0.86	1.76*	
12	activin beta E	Inhbe	AF089825	cell signaling, extracellular communication proteins	1.35*	0.89	0.72*	
20	ribosomal protein L6	Rpl6	X87107	translation	1.99	1.96	2.01*	0.00040
20	N-Acetyltransferase-2	Nat2	U17261	stress response proteins	0.61	0.48*	0.53*	0.00047
20	Cathepsin L	Ctsl	Y00697	protein turnover	1.12	1.33	1.63*	
20	angiotensinogen	Agt	L00091	protein turnover	0.38	0.22*	0.38*	0.00039
20	cyclin D1	Ccnd1	D14014	oncogenes and tumor suppressors	0.34	0.41*	2*	
20	UDP-glucuronosyltransferase	Ugt2b4	U06273	metabolism	1.48	1.97*	1.34*	0.00051
20	enolase 1, alpha	Eno1	X02610	metabolism	1.43	1.98*	1.28*	
20	hypoxanthine guanine phosphoribosyl transferase	Hprt	M63983	metabolism	1.78	2.04*	1.24*	0.00049
20	glutamic-pyruvate transaminase (alanine aminotransferase)	Gpt1	D10354	metabolism	0.6	0.43*	0.64*	0.00048
20	cytochrome P-450PCN (PNCN inducible)	Cyp3a1	M10161	metabolism	0.69	0.44*	0.28*	0.00043
20	Aldehyde dehydrogenase family 3, subfamily A1	Aldh3a1	J03637	metabolism	0.69	4.33*	4.52*	0.00069
20	NAD(P)H dehydrogenase, quinone 1	Nqo1	J02608	metabolism	2.02	3.79*	4.97*	0.00048
20	Sterol carrier protein 2, liver	Scp2	M34728	metabolism	0.92	0.71*	0.59*	
20	UDP glycosyltransferase 1 family, polypeptide A7	Ugt1a7	U75903	metabolism	1.74	3.01*	6.1*	0.00051
20	alkaline phosphatase, tissue-nonspecific	Alpl	J03572	metabolism	0.48	0.46*	1.85*	
20	3-hydroxy-3-methylglutaryl-Coenzyme A synthase 2	Hmgcs2	M33648	metabolism	0.38	0.21*	0.66*	0.00040
20	glutamate cysteine ligase, modifier subunit	Gclm	L22191	metabolism	1.26	2.42*	4.59*	0.00040
20	Fatty acid binding protein 1, liver	Fabp1	M35991	intracellular transducers/ effectors/modulators	0.68	0.48*	0.33*	0.00052
20	MHC class I-related protein (MR1)		Y13972	immune system proteins	0.7	0.33*	0.52*	0.00041
20	Amiloride binding protein 1	Abp1	X73911	extracellular transport/ carrier proteins	0.54	0.61*	0.56*	0.00032
22	nuclear factor I/A	Nfia	D78017	transcription	0.57*	0.64	0.93	0.00051
22	alpha thalassemia/mental retardation syndrome X-linked (RAD54 homolog, S.cerevisiae)	Atrx	D64059	transcription	0.49*	0.56	0.89	0.00040
22	Fos like antigen 2	Fosl2	U18913	transcription	0.45*	0.76	0.79	0.00042
22	Early growth response 1	Egr1	M18416	transcription	0.44*	0.48	0.78	0.00051
22	protein disulfide isomerase-related protein	Txndc7	X79328	trafficking/targeting proteins	2.05*	2.71	0.85	
22	ADP-ribosylation factor 3	Arf3	L12382	trafficking/targeting proteins	0.62*	0.77	1.22	
22	ATP-binding cassette, sub-family C (CFTR/MRP), member 2	Abcc2	L49379	stress response proteins	0.4*	0.66	1.21	
22	acidic ribosomal protein P0	Arbp	Z29530	RNA processing, turnover, and transport	2.97*	1.87	1.23	0.00053
22	CDC-like kinase 3	Clk3	X94351	RNA processing, turnover, and transport	0.46*	0.52	0.76	0.00042
22	stress-induced-phosphoprotein 1 (Hsp70/Hsp90-organizing protein)	Stip1	Y15068	post-translational modification/protein folding	0.56*	0.71	1.3	
22	dihydropyrimidine dehydrogenase	Dpyd	D85035	metabolism	2.89*	1.9	0.77	
22	arachidonic acid epoxygenase	Cyp2c23	X55446	metabolism	1.63*	1	0.54	

Table W1. (*continued*)

Venn Section	Gene Name	Symbol	Genbank	Functional Classification	Ratio			FDR
					ENT1/NL	ENT5/L	HCC/NL	
22	cytochrome P450, 1a1	Cyp1a1	X00469	metabolism	2.96*	1.24	0.56	
22	sodium channel, voltage-gated, type 1, beta polypeptide	Scn1b	M91808	membrane channels and transporters	0.38*	0.5	1.13	0.00076
22	ATPase, Ca++ transporting, cardiac muscle, slow twitch 2	Atp2a2	J04022	membrane channels and transporters	0.43*	0.58	0.79	0.00045
22	phosphodiesterase 3B	Pde3b	Z22867	intracellular transducers/ effectors/modulators	0.49*	0.59	0.73	
22	Transferrin	Tf	D38380	extracellular transport/ carrier proteins	1.6*	1.48	0.9	0.00048
22	insulin-like growth factor 1	Igf1	M15480	cell signaling, extracellular communication proteins	2.53*	1.3	0.48	
22	kinase substrate HASPP28	Pdap1	U41744	cell signaling, extracellular communication proteins	0.63*	0.77	1.4	
22	Follicle stimulating hormone receptor	Fshr	L02842	cell receptors (by ligands)	0.42*	0.6	1	0.00039
22	transforming growth factor, beta receptor 3	Tgfbr3	M77809	cell receptors (by ligands)	0.36*	0.63	0.71	0.00044
22	nuclear receptor subfamily 2, group F, member 6	Nr2f6	AF003926	cell receptors (by activities)	0.63*	0.77	0.86	0.00045
40	ribosomal protein S5	Rps5	X58465	translation	4.27*	4.95*	1.39*	0.00040
40	nuclear factor of kappa light chain gene enhancer in B-cells inhibitor, alpha	Nfkbia	X63594	transcription	0.48*	0.59*	1.19*	
40	Inhibitor of DNA binding 3, dominant negative helix-loop-helix protein	Id3	D10864	transcription	0.42*	0.39*	1.56*	
40	Apolipoprotein E	Apoe	J02582	trafficking/targeting proteins	0.21*	0.2*	0.8*	0.00040
40	glutathione S-transferase, alpha 1	Gsta5	K01932	stress response proteins	3*	3.82*	2.01*	0.00038
40	Metallothionein	Mt1a	J00750	stress response proteins	5.08*	2.29*	0.55*	0.00186
40	glutathione-S-transferase, alpha type2	Gsta2	K01931	stress response proteins	5.29*	7.08*	2.8*	0.00011
40	solute carrier family 21, member 1	Slc21a1	L19031	stress response proteins	0.49*	0.44*	0.28*	0.00042
40	endothelin converting enzyme 1	Ece1	D29683	protein turnover	0.35*	0.4*	0.8*	0.00046
40	Glutathione peroxidase 1	Gpx1	X12367	protein turnover	0.54*	0.41*	0.54*	0.00031
40	glucose regulated protein, 58 kDa	Grp58	D63378	protein turnover	0.24*	0.4*	0.85*	0.00040
40	protein disulfide isomerase related protein (calcium-binding protein, intestinal-related)	Erp70	M86870	post-translational modification/ protein folding	0.42*	0.62*	0.65*	0.00049
40	Superoxide dismutase 2, mitochondrial	Sod2	X56600	metabolism	0.4*	0.62*	1.14*	
40	fatty acid Coenzyme A ligase, long chain 2	Acsl1	D90109	metabolism	0.64*	0.43*	0.45*	0.00052
40	glycerol kinase	Gyk	D16102	metabolism	0.31*	0.34*	0.46*	0.00031
40	glutathione S-transferase, mu type 3 (Yb3)	Gstm3	J02744	metabolism	3.78*	4.86*	2.48*	0.00018
40	peroxiredoxin 5	Prdx6	Y17295	metabolism	2.35*	2.5*	1.65*	0.00049
40	sulfotransferase, estrogen preferring	Ste	M86758	metabolism	0.5*	0.53*	0.15*	0.00043
40	alcohol dehydrogenase 1	Adh1	M15327	metabolism	10.66*	11.57*	3.74*	0.00041
40	glutathione S-transferase, pi 1	Gstp1	X02904	metabolism	13.59*	21.89*	22.76*	0.00003
40	glutamate-cysteine ligase, catalytic subunit	Gclc	J05181	metabolism	2.28*	4.05*	7.22*	0.00012
40	aldehyde dehydrogenase family 1, subfamily A4	Aldh1a4	M23995	metabolism	4.24*	6.76*	4.22*	0.00031
40	phosphoenolpyruvate carboxykinase		K03243	metabolism	0.43*	0.22*	0.24*	0.00011
40	carbonic anhydrase 3	Ca3	M22413	metabolism	0.3*	0.19*	0.2*	0.00010
40	acyl-Coenzyme A oxidase 2, branched chain	Acox2	X95189	metabolism	0.31*	0.29*	0.27*	0.00009
40	Phosphoinositide 3-kinase, regulatory subunit, polypeptide 1 (p85 alpha)	Pik3r1	D64045	intracellular transducers/ effectors/modulators	0.35*	0.27*	0.65*	0.00040
40	GTP-binding protein (G-alpha-i2)	Gnai2	M17528	intracellular transducers/ effectors/modulators	0.44*	0.6*	1.72*	
40	guanine nucleotide binding protein, alpha 12	Gna12	D85760	intracellular transducers/ effectors/modulators	0.33*	0.42*	1.48*	
40	cold shock domain protein A	Csda	U22893	DNA binding and chromatin proteins	0.57*	0.64*	1.96*	
40	leukemia inhibitory factor	Lif	M32748	cell signaling, extracellular communication proteins	0.34*	0.23*	0.46*	0.00040
40	hepatocyte growth factor	Hgf	D90102	cell signaling, extracellular communication proteins	0.48*	0.54*	0.67*	0.00031
40	interleukin 6 receptor	Il6r	M58587	cell receptors (by ligands)	0.24*	0.17*	0.37*	0.00040
40	Interleukin 1 receptor, type 1	Il1r1	M95578	cell receptors (by ligands)	0.33*	0.26*	0.5*	0.00020
40	epidermal growth factor receptor	Egfr	M37394	cell receptors (by ligands)	0.43*	0.43*	0.52*	0.00012
40	Retinoid X receptor alpha	Rxra	L06482	cell receptors (by ligands)	0.17*	0.21*	0.7*	0.00042

Table W1. (*continued*)

Venn Section	Gene Name	Symbol	Genbank	Functional Classification	Ratio			FDR
					ENT1/NL	ENT5/L	HCC/NL	
40	Integrin, beta 1	Itgb1	U12309	cell receptors (by ligands)	2.15*	2.42*	1.29*	0.00042
40	ribosomal protein L24	Rp124	X78443		2.72*	3.12*	1.44*	0.00046
40	cytochrome P450, 8b1, sterol 12 alpha-hydrolase	Cyp8b1	AB018596		0.47	0.26*	0.29*	0.00039
43	rap7a	Dap	U05334		2.56*	3.81*	2.73*	0.00006
43	probasin	Pbsn	M27156		0.46*	0.48*	0.58*	0.00012
43	retinoblastoma binding protein 7	Rbbp7	AF090306	transcription	0.58	0.59*	1.19	
43	nuclear factor I/X	Nfix	AB012234	transcription	0.47	0.48*	0.83	0.00042
43	alpha1-antitrypsin promoter binding protein 2 (ATBP2)	Hivep1	X54250	transcription	0.42	0.47*	0.81	0.00040
43	Retinoblastoma-related gene	Rbl2	D55627	transcription	0.44	0.48*	0.77	0.00049
43	heat shock 10 kDa protein 1	Hspe1	X71429	stress response proteins	1.54	1.85*	0.9	
43	T-complex 1	Tcp1	D90345	stress response proteins	0.88	1.2*	1.14	
43	growth arrest and DNA-damage-inducible 45 alpha	Gadd45a	L32591	stress response proteins	0.42	0.34*	0.8	0.00045
43	Finkel-Biskis-Reilly murine sarcoma virusubiquitously expressed	Fau	X62671	protein turnover	0.49	0.41*	1.2	0.00070
43	Peptidylprolyl isomerase A (cyclophilin A)	Ppia	M19533	post-translational modification/ protein folding	1.56	2.45*	1.16	
43	suppression of tumorigenicity 13 (colon carcinoma) Hsp70-interacting protein	St13	X82021	post-translational modification/ protein folding	1.23	2.02*	1.66	0.00040
43	avian sarcoma virus CT10 (v-crk) oncogene homolog	Crk	D44481	oncogenes and tumor suppressors	0.38	0.29*	1.07	0.00045
43	Kirsten rat sarcoma viral oncogene homologue 2 (active)	Kras2	U09793	oncogenes and tumor suppressors	0.55	0.47*	1.24	
43	Superoxide dismutase 1, soluble	Sod1	Y00404	metabolism	0.51	0.39*	0.92	0.00040
43	acyl-coenzyme A:cholesterol acyltransferase	Soat1	D86373	metabolism	0.42	0.36*	0.76	0.00050
40	liver UDP-glucuronosyltransferase, phenobarbital inducible form	Udpgtr2	M13506	metabolism	0.88	0.3*	0.17	0.00040
40	peroxiredoxin 1	Prdx1	D30035	metabolism	1.67	2.56*	1.55	0.00039
43	mel transforming oncogene (derived from cell line NK14)- RAB8 homolog	Rab8a	M83675	intracellular transducers/ effectors/modulators	0.49	0.58*	0.99	0.00048
43	Protein phosphatase 2 (formerly 2A), catalytic subunit, alpha isoform	Ppp2ca	X16043	intracellular transducers/ effectors/modulators	2.1	2.86*	1.05	0.00118
43	mitogen activated protein kinase 1	Mapk1	M64300	intracellular transducers/ effectors/modulators	0.36	0.4*	1.11	0.00082
43	GTPase Rab14	Rab14	M83680	intracellular transducers/ effectors/modulators	0.46	0.44*	0.89	0.00039
43	calmodulin 3	Calm3	X13817	intracellular transducers/ effectors/modulators	2.27	3.82*	1.36	0.00052
43	adrenergic receptor, alpha 2c	Adra2c	M58316	cell receptors (by ligands)	0.52	0.55*	0.9	0.00043
43	insulin-like growth factor 1 receptor	Igf1r	L29232	cell receptors (by ligands)	0.5	0.4*	0.92	0.00041
43	nuclear receptor subfamily 1, group H, member 4	Nr1h4	U18374	cell receptors (by ligands)	0.66	0.52*	0.89	
43	G protein-coupled receptor 27; gustatory receptor 27 (GUST27)	Olr1867	D12820	cell receptors (by ligands)	0.55	0.38*	0.77	0.00046
43	parathyroid hormone receptor	Pthr1	L19475	cell receptors (by ligands)	0.52	0.5*	0.71	0.00045
43	defender against cell death 1	Dad1	Y13336	cell receptors (by ligands)	1.16	1.66*	1.15	0.00051
43	galanin receptor 1	Galr1	U30290	cell receptors (by ligands)	0.71	0.62*	0.77	0.00046
43	leukemia inhibitor factor receptor alpha-chain	Lifr	D86345	cell receptors (by ligands)	0.62	0.39*	0.57	0.00049
43	5-hydroxytryptamine (serotonin) receptor 2B	Htr2b	X66842	cell receptors (by ligands)	0.45	0.48*	0.58	0.00046
43	androgen receptor	Ar	M20133	cell receptors (by activities)	0.46	0.55*	0.73	0.00045
43	cyclin-dependent kinase inhibitor 1B	Cdkn1b	D83792	cell cycle	0.45	0.45*	0.85	0.00041
43	small GTP-binding protein rab5	Rab5a	AF072935		0.4	0.45*	0.95	
43	notch gene homolog 2, (Drosophila)	Notch2	M93661		0.65	0.67*	0.95	
43	Secreted acidic cystein-rich glycoprotein (osteonectin)	Sparc	Y13714		0.7	0.58*	0.9	
43	Sp1 transcription factor	Sp1	D12768		0.36	0.44*	0.87	0.00042
43	thioredoxin	Txn1	X14878		1.74	2.23*	1.19	0.00045
43	collagen, type III, alpha 1	Col3a1	M21354		0.87	0.55*	0.86	
43	high mobility group AT-hook 1	Hmga1	X62875		0.52	0.52*	0.78	0.00045
43	profilin	Pfn1	X96967		1.44	1.69*	1.32	
43	non-muscle myosin alkali light chain		S77858		2.41	2.64*	1.28	0.00040
43	CCAAT/enhancer binding protein, gamma	Cebpg	X64403		0.36	0.31*	0.67	0.00041
43	epidermal growth factor	Egf	U04842		0.82	0.55*	0.68	0.00046
69	ribosomal protein S9	Rps9	X66370	translation	4.72*	4.5*	1.35	0.00039

Table W1. (*continued*)

Venn Section	Gene Name	Symbol	Genbank	Functional Classification	Ratio			FDR
					ENT1/NL	ENT5/L	HCC/NL	
69	ribosomal protein S3	Rps3	X51536	translation	4.7*	5.08*	1.28	0.00049
69	nucleophosmin 1	Npm1	J03969	translation	2.09*	2.63*	1.49	0.00045
69	hepatocyte nuclear factor 4, alpha	Hnf4a	D10554	transcription	0.24*	0.22*	0.81	0.00040
69	zinc finger protein 36	Zfp36	X63369	transcription	0.34*	0.34*	0.8	0.00040
69	presenilin 1	Psen1	D82363	trafficking/targeting proteins	0.29*	0.31*	1.08	0.00046
69	ATP-binding cassette, sub-family B (MDR/TAP), member 4	Abcb4	L15079	stress response proteins	0.3*	0.29*	0.71	0.00046
69	solute carrier family 22, member 5	Slc22a5	AJ001933	stress response proteins	4.5*	6.32*	0.73	
69	heat shock 70kD protein 8		Y00054	stress response proteins	2.79*	2.99*	1.51	0.00040
69	tissue inhibitor of metalloproteinase 2	Timp2	L31884	protein turnover	0.46*	0.48*	0.97	0.00041
69	cathepsin B	Ctsb	X82396	protein turnover	3.04*	3*	1.07	0.00067
69	polyubiquitin	Ubb	D16554	protein turnover	0.36*	0.43*	0.95	0.00043
69	ubiquitin conjugating enzyme	Ube2b	M62388	protein turnover	0.43*	0.42*	0.6	0.00048
69	carboxypeptidase D	Cpd	U62897	protein turnover	0.58*	0.53*	1.13	
69	P450 (cytochrome) oxidoreductase	Por	M12516	post-translational modification/ protein folding	0.36*	0.27*	1.07	0.00078
69	chaperonin containing TCP1, subunit 3 (gamma)		X74801	post-translational modification/ protein folding	3.41*	4*	0.91	0.00111
69	H-ras proto-oncogene; transforming protein p21		M13011	oncogenes and tumor suppressors	0.37*	0.37*	0.96	0.00053
69	cyclin D2	Ccnd2	D16308	oncogenes and tumor suppressors	0.42*	0.43*	0.94	0.00040
69	phosphoglycerate kinase 1	Pgk1	M31788	metabolism	2.03*	2.14*	1.02	
69	cytochrome P450, 4a12	Cyp4a12	M37828	metabolism	2.43*	2.73*	1.1	0.00042
69	cytochrome c oxidase, subunit 4a	Cox4i1	X14209	metabolism	0.66*	0.68*	0.98	
69	7-dehydrocholesterol reductase	Dhcr7	AB016800	metabolism	2.9*	3.49*	1.14	0.00109
69	heme oxygenase 2	Hmox2	J05405	metabolism	0.49*	0.43*	0.86	0.00041
69	dopa/tyrosine sulfotransferase	Sult1b1	U38419	metabolism	1.53*	1.6*	0.88	
69	biliverdin reductase A	Blvra	M81681	metabolism	0.38*	0.47*	0.93	0.00049
69	Apolipoprotein A-IV	Apoa4	M00002	metabolism	0.18*	0.09*	0.68	0.00041
69	cytosolic acyl-CoA thioesterase 1	Cte1	AB010428	metabolism	0.32*	0.39*	1.27	0.00119
69	transferrin receptor	Tfrc	M58040	metabolism	1.37*	1.18*	1.27	
69	mitochondrial H+-ATP synthase alpha subunit	Atp5a1	X56133	metabolism	4.06*	3.61*	1.15	0.00043
69	carnitine palmitoyltransferase 1	Cpt1a	L07736	metabolism	0.25*	0.34*	0.71	0.00040
69	Glyceraldehyde-3-phosphate dehydrogenase	Gapd	M17701	metabolism	1.93*	2.04*	1.24	0.00051
69	cytochrome c oxidase subunit Vb	Cox5b	D10952	metabolism	0.2*	0.22*	0.76	0.00040
69	ATP-binding cassette, sub-family B (MDR/TAP), member 6	Abcb6	AJ003004	membrane channels and transporters	1.42*	2.19*	0.94	
69	inositol 1,4,5-triphosphate receptor type 1	Itpr1	U38665	membrane channels and transporters	0.41*	0.38*	0.75	0.00040
69	A-raf	Araf1	X06942	intracellular transducers/ effectors/modulators	0.46*	0.56*	1	0.00052
69	mitogen activated protein kinase kinase 2	Map2k2	D14592	intracellular transducers/ effectors/modulators	0.37*	0.42*	1.08	0.00061
69	p38 mitogen activated protein kinase	Mapk14	U73142	intracellular transducers/ effectors/modulators	0.33*	0.38*	1.14	0.00069
69	RAS p21 protein activator 1	Rasa1	L13151	intracellular transducers/ effectors/modulators	0.42*	0.46*	1.16	0.00046
69	Murine thymoma viral (v-akt) oncogene homolog 2	Akt2	D30041	intracellular transducers/ effectors/modulators	0.4*	0.39*	0.82	0.00044
69	mitogen-activated protein kinase 6	Mapk6	M64301	intracellular transducers/ effectors/modulators	0.47*	0.44*	1.22	
69	Insulin receptor substrate 1	Irs1	X58375	intracellular transducers/ effectors/modulators	0.39*	0.49*	0.76	0.00046
69	insulin-like growth factor binding protein 1	Igfbp1	M89791	extracellular transport/ carrier proteins	2.46*	2.5*	1.11	0.00059
69	insulin-like growth factor binding protein 3	Igfbp3	M31837	extracellular transport/carrier proteins	0.4*	0.61*	2.07	
69	8-oxoguanine-DNA-glycosylase	Ogg1	AF029690	DNA synthesis, recombination, and repair	0.48*	0.67*	1.04	
69	histone 2A	H2a	U95113	DNA binding and chromatin proteins	0.18*	0.23*	1.05	0.00070
69	vimentin	Vim	X62952	cytoskeleton/motility proteins	0.48*	0.43*	1	0.00039
69	alpha-tubulin	Tuba1	V01227	cytoskeleton/motility proteins	1.78*	2.24*	1.06	
69	fibroblast growth factor 10	Fgf10	D79215	cell signaling, extracellular communication proteins	4.09*	4.24*	1.37	0.00079
69	Glucose-dependent insulinotropic peptide	Gip	L08831	cell signaling, extracellular communication proteins	5.69*	4.04*	1.99	0.00052

Table W1. (*continued*)

Venn Section	Gene Name	Symbol	Genbank	Functional Classification	Ratio			FDR
					ENT1/NL	ENT5/L	HCC/NL	
69	vascular endothelial growth factor	Vegfa	M32167	cell signaling, extracellular communication proteins	0.34*	0.42*	1.16	0.00065
69	interleukin 4 receptor	Il4r	X69903	cell receptors (by ligands)	0.26*	0.34*	0.89	0.00040
69	met proto-oncogene	Met	U65007	cell receptors (by ligands)	0.34*	0.36*	0.66	0.00045
69	insulin receptor	Insr	M29014	cell receptors (by ligands)	0.37*	0.42*	0.74	0.00052
69	natriuretic peptide receptor 1	Npr1	M74535	cell receptors (by ligands)	0.36*	0.44*	0.66	0.00052
69	growth hormone receptor	Ghr	J04811	cell receptors (by ligands)	0.41*	0.35*	0.56	0.00050
69	Low density lipoprotein receptor	Ldlr	X13722	cell receptors (by ligands)	0.43*	0.42*	0.62	0.00032
69	Peroxisome proliferator activated receptor alpha	Ppara	M88592	cell receptors (by activities)	0.26*	0.38*	0.94	0.00050
69	nuclear receptor subfamily 1, group D, member 1	Nr1d1	M25804	cell receptors (by activities)	0.24*	0.35*	0.71	0.00045
69	Cyclin D3	Ccnd3	D16309	cell cycle	0.31*	0.31*	0.81	0.00043
69	tenascin		U15550	cell adhesion receptors/ proteins	0.55*	0.58*	0.9	0.00046
69	tumor necrosis factor receptor superfamily, member 1	Tnfrsf1a	M63122	apoptosis associated proteins	0.23*	0.23*	1.05	0.00047
69	B cell lymphoma 2 like	Bcl2l1	U72350	apoptosis associated proteins	0.3*	0.32*	0.81	0.00040
69	myeloid cell leukemia sequence 1	Mcl1	AF115380	apoptosis associated proteins	0.62*	0.44*	1.14	
69	UDP-glucuronosyltransferase 1 family, member 1	Ugt1a1	U20551		0.49*	0.45*	0.88	0.00039
69	cytochrome bc-1 complex core P		S74321		1.69*	1.57*	1.13	
69	cell growth regulatory with ring finger domain	Cgrrf1	U66471		0.38*	0.45*	0.78	0.00044
69	K-kininogen, differential splicing leads to HMW Kngk	Kng_v1	L29428		3.58*	3.49*	1.4	0.00043
69	nuclear factor kappa B subunit p65 (NFkB)		AF079314		0.39*	0.48*	1.24	0.00095
69	metallothionein 3	Mt3	S65838		5.56*	2.52*	0.78	0.00128
69	17-beta hydroxysteroid dehydrogenase type 2	Hsd17b2	X91234		0.72	0.8	0.5*	0.00052
69	actin, beta	Actb	V01217	cytoskeleton/motility proteins	0.85	0.72	1.27*	
69	aldehyde dehydrogenase family 3, subfamily A2	Aldh3a2	M73714	metabolism	1.41	0.98	0.63*	
84	alpha-2-HS-glycoprotein	Ahsg	X63446	intracellular transducers/ effectors/modulators	0.98	0.45	0.43*	0.00045
84	alpha-2-macroglobulin	A2m	J02635	protein turnover	1.07	0.65	2.46*	
84	annexin 1	Anxa1	M19967	metabolism	0.93	2.75	5.02*	0.00053
84	annexin 5	Anxa5	M21730	intracellular transducers/ effectors/modulators	1.39	1.43	3.63*	0.00039
84	Apolipoprotein A-II	Apoa2	X03468		1.16	0.65	0.32*	
84	apurinic/apyrimidinic endonuclease 1	Apex1	D44495	DNA synthesis, recombination, and repair	0.66	0.66	1.56*	
84	aquaporin 8	Aqp8	AF007775	membrane channels and transporters	1.79	4.14	1.77*	0.00040
84	arginase 1	Arg1	J02720	metabolism	1.3	0.72	0.49*	
84	arginosuccinate synthetase 1	Ass	M36708	metabolism	0.76	0.47	0.31*	0.00044
84	ATP-binding cassette, sub-family C (CFTR/MRP), member 3	Abcc3	AB010467	stress response proteins	0.7	0.84	1.52*	
84	Benzodiazepin receptor (peripheral)	Bzrp	M84221	cell receptors (by ligands)	0.89	1.4	1.8*	
84	betaine-homocysteine methyltransferase	Bhmt	AF038870	metabolism	1.19	0.75	0.28*	0.00089
84	calnexin	Canx	L18889	intracellular transducers/ effectors/modulators	0.9	0.94	0.71*	
84	calreticulin	Calr	X53363	intracellular transducers/ effectors/modulators	0.69	0.76	0.77*	
84	CD24 antigen	Cd24	U49062	cell adhesion receptors/ proteins	1.05	0.93	1.53*	
84	cell division cycle 42 homolog (S. cerevisiae)	Cdc42	M35543	intracellular transducers/ effectors/modulators	2.39	3.4	1.27*	0.00090
84	C-reactive protein	Crp	M83176	cell signaling, extracellular communication proteins	1.38	0.78	0.32*	0.00099
84	crystallin, beta B2	Crybb2	X16072	stress response proteins	0.49	0.65	0.65*	0.00041
84	cytochrome P450 2B1	Cyp2b1	M11251	metabolism	1.17	0.88	0.65*	
84	Cytochrome P450 IIA1 (hepatic steroid hydroxylase IIA1) gene	Cyp2a1	J02669	metabolism	0.83	0.39	0.34*	0.00039
84	cytochrome P450, 1a2	Cyp1a2	K02422	metabolism	1.52	0.66	0.22*	0.00088
84	cytochrome P450, 7a1	Cyp7a1	J05460	metabolism	0.97	0.61	0.33*	0.00046
84	cytochrome P450, subfamily 17	Cyp17a1	M21208	metabolism	1.02	0.54	0.54*	0.00040
84	cytochrome P450, subfamily 27b, polypeptide 1	Cyp27b1	AB001992	metabolism	0.65	0.99	0.63*	0.00040

Table W1. (*continued*)

Venn Section	Gene Name	Symbol	Genbank	Functional Classification	Ratio			FDR
					ENT1/NL	ENT5/L	HCC/NL	
84	diazepam binding inhibitor	Dbi	M14201		1.57	1.28	0.6*	
84	Discoidin domain receptor family, member 1	Ddr1	L26525	cell receptors (by activities)	0.71	0.75	5.03*	
84	DNA polymerase beta	Polb	J02776	DNA synthesis, recombination, and repair	0.54	0.74	0.68*	0.00039
84	enoyl Coenzyme A hydratase, short chain 1	Echs1	X15958	metabolism	1.69	1.42	0.69*	
84	eukaryotic translation elongation factor 2	Eef2	K03502	translation	0.75	0.52	1.29*	
84	fatty acid binding protein 5, epidermal	Fabp5	U13253	metabolism	2.38	1.69	1.93*	0.00046
84	Fibrinogen, gamma polypeptide	Fgg	J00734		1.46	0.89	0.52*	
84	Fibronectin 1	Fn1	X05834	extracellular matrix proteins	0.94	0.78	0.49*	0.00044
84	Flavin-containing monooxygenase 1	Fmo1	M84719	stress response proteins	0.87	0.56	0.52*	0.00040
84	fructose-1,6-bisphosphatase 1	Fbp1	M86240	metabolism	1.39	1.05	0.51*	
84	gamma-glutamyl hydrolase	Ggh	U38379	metabolism	0.75	0.89	1.35*	
84	gamma-glutamyl transpeptidase	Ggt1	M33821	metabolism	1.06	1.25	3.33*	0.00097
84	gastric inhibitory peptide receptor	Gipr	L19660	cell receptors (by ligands)	0.82	0.93	0.67*	
84	glucose-6-phosphate dehydrogenase	G6pdx	X07467	metabolism	1.6	2.92	3.42*	0.00050
84	glutamate oxaloacetate transaminase 1	Got1	J04171	metabolism	0.84	0.44	0.29*	0.00040
84	glutathione reductase	Gsr	U73174	metabolism	0.97	1.57	2.35*	
84	glutathione synthetase	Gss	L38615	metabolism	0.55	0.68	2.62*	
84	glycine transporter 1	Slc6a9	M88595	membrane channels and transporters	0.44	0.69	2.39*	
84	guanine nucleotide binding protein, alpha o	Gnao	M17526	intracellular transducers/ effectors/modulators	0.49	0.42	0.42*	0.00048
84	Huntington disease gene homolog	Hdh	U18650	trafficking/targeting proteins	1.09	0.53	0.6*	0.00108
84	hydroxy-delta-5-steroid dehydrogenase, 3 beta- and steroid delta-isomerase	Hsd3b	M67465	metabolism	0.54	0.51	0.36*	0.00040
84	hydroxy-delta-5-steroid dehydrogenase, 3 beta- and steroid delta-isomerase 1	Hsd3b1	M38178	metabolism	1.09	1.27	0.49*	
84	hydroxysteroid dehydrogenase 17 beta, type 7	Hsd17b7	U44803	intracellular transducers/ effectors/modulators	1.1	0.91	0.71*	
84	Inhibitor of DNA binding 2, dominant negative helix-loop-helix protein	Id2	D10863	transcription	0.86	0.72	2.24*	
84	lactate dehydrogenase B	Ldhb	U07181	metabolism	0.63	0.92	1.94*	
84	laminin receptor 1 (67kD, ribosomal protein SA)	Lamr1	D25224		2.49	1.74	1.65*	0.00065
84	Male germ cell-associated kinase	Mak	M35862	intracellular transducers/ effectors/modulators	0.74	0.85	1.36*	
84	mitogen-activated protein kinase 12	Mapk12	X96488	intracellular transducers/ effectors/modulators	0.65	0.47	0.55*	0.00039
84	mouse double minute 2, human homolog of; p53-binding protein		Z12020	transcription	0.53	0.65	1.61*	
84	neuropilin-2	Nrp2	AF016297	cell receptors (by ligands)	0.75	0.98	1.84*	
84	O6-methylguanine-DNA methyltranferase	Mgmt	X54862	DNA synthesis, recombination, and repair	0.93	1.23	0.76*	
84	phospholipase A2, group VI	Pla2g6	U51898	metabolism	0.48	0.75	1.62*	
84	pre-alpha inhibitor heavy chain 3	Itih3	X83231	protein turnover	1.74	1.42	0.58*	
84	Prion protein, structural	Prnp	D50093		0.94	0.87	1.74*	
84	protein kinase inhibitor, alpha	Pkia	L02615	intracellular transducers/ effectors/modulators	0.72	0.94	2.08*	
84	Protein phosphatase 2 (formerly 2A), catalytic subunit, beta isoform	Ppp2cb	M23591	intracellular transducers/ effectors/modulators	0.84	1.06	1.99*	
84	Regucalcin	Rgn	D38467	intracellular transducers/ effectors/modulators	1.36	0.74	0.31*	0.00089
84	ribosomal protein L15	Rpl15	X78167	translation	0.95	0.75	1.32*	
84	ribosomal protein L3	Rpl3	X62166		1.25	0.94	1.32*	
84	serine (or cysteine) proteinase inhibitor, clade H, member 1	Serpinh1	M69246	stress response proteins	0.52	0.42	2.14*	
84	Serine protease inhibitor	Spin2c	D00753	protein turnover	1.23	1.18	0.75*	
84	serine protease inhibitor 2.4	Serpina3m	X69834	protein turnover	1.05	0.92	0.39*	
84	signal transducer and activator of transcription 1	Stat1	AF205604		1.08	1.07	0.64*	
84	sodium-dependent neutral amino acid transporter ASCT2	Slc1a5	AJ132846	membrane channels and transporters	0.53	0.72	0.61*	0.00043
84	solute carrier family 17 vesicular glutamate transporter), member 1	Slc17a1	U28504	membrane channels and transporters	1.47	3.33	3.6*	0.00049

Table W1. (*continued*)

Venn Section	Gene Name	Symbol	Genbank	Functional Classification	Ratio			FDR
					ENT1/NL	ENT5/L	HCC/NL	
84	solute carrier family 25 (mitochondrial adenine nucleotide translocator) member 4	Slc25a4	D12770	metabolism	1.73	1.3	1.53*	
84	syndecan 2	Sdc2	M81687		0.59	0.45	0.66*	0.00044
84	testis-specific heat shock protein-related gene hst70	Hspa2	X15705	stress response proteins	0.45	0.55	0.52*	0.00047
84	thioredoxin reductase 1	Txnrd1	AF220760		1.15	2.3	3.88*	0.00043
84	thymosin, beta 10	Tmsb10	M17698		1.05	1.12	4.79*	0.00073
84	thyroid hormone receptor alpha	Thra	X12744,M31177	oncogenes and tumor suppressors	0.61	0.62	0.75*	0.00039
84	tyrosine 3-monooxgenase/tryptophan 5-monooxgenase activation protein, gamma polypeptide	Ywhag	S55305	metabolism	1.02	1.35	2.04*	
84	Tyrosine 3-monooxygenase 5-monooxygenase activation protein, eta polypeptide	Ywhah	D17445	metabolism	0.53	0.92	1.54*	
84	Tyrosine 3-monooxygenase 5-monooxygenase activation protein, zeta polypeptide	Ywhaz	D17615	metabolism	0.51	0.71	1.66*	
84	tyrosine aminotransferase	Tat	M18340	metabolism	0.7	0.46	0.2*	0.00042
84	urate oxidase	Uox	J03959	metabolism	1.66	0.86	0.36*	
84	zinc finger protein 354A	Znf354a	M96548	transcription	0.52	0.37	0.22*	0.00048

Full list of differential genes classified according to Venn diagram (Figure 2).
*Ratios are statistically different compared with NL ($P \leq .05$).

Table W2. Functional Classificafion of the 290 Differential Genes.

Functional Classification	Number of Genes	% of Genes
apoptosis associated proteins	3	1.0
cell adhesion receptors/proteins	2	0.7
cell cycle	2	0.7
cell receptors	31	10.7
cell signaling, extracellular communication proteins	9	3.1
cytoskeleton/motility proteins	4	1.4
DNA binding and chromatin proteins	2	0.7
DNA synthesis, recombination, and repair	4	1.4
extracellular matrix proteins	1	0.3
extracellular transport/carrier proteins	4	1.4
immune system proteins	2	0.7
intracellular transducers/effectors/modulators	30	10.3
membrane channels and transporters	8	2.8
metabolism	80	27.6
oncogenes and tumor suppressors	6	2.1
post-translational modification/protein folding	6	2.1
protein turnover	17	5.9
RNA processing, turnover, and transport	2	0.7
stress response proteins	18	6.2
trafficking/targeting proteins	6	2.1
transcription	15	5.2
translation	7	2.4
unclassified	31	10.7
	290	100